J Mater Sci (2017) 52:6173–6195

Review

Electrospun porous nanofibers for electrochemical energy storage

Zhi Li[1,2], Ji-wei Zhang[1,2,*], Lai-gui Yu[1,2], and Jing-wei Zhang[1,2,*]

[1] National and Local Joint Engineering Research Center for Applied Technology of Hybrid Nanomaterials, Henan University, Kaifeng 475004, People's Republic of China
[2] Collaborative Innovation Center of Nano Functional Materials and Applications of Henan Province, Henan University, Kaifeng 475004, People's Republic of China

Received: 9 October 2016
Accepted: 12 January 2017
Published online: 25 January 2017

ABSTRACT

The demand for energy storage systems is rising due to the rapid development of electric transportation vehicles, and this demand is stimulating research on the next generation of high-performance, high-density energy storage devices. In this work, nanomaterials with excellent electrochemical properties are of particular significance. This review summarizes a variety of methods based on electrospinning techniques for the preparation of porous nanofibers with controllable morphologies. An emphasis is placed on methods involving polymer templates and polymer blend templates, hard templates, and on solvent-induced, nonsolvent-induced or activation methods. As a simple and cost-effective method for preparing one-dimensional nanomaterials, the electrospinning technique is of special significance in the energy storage field, because the as-prepared porous nanofibers exhibit large specific surface areas and interconnected micro-/meso-/macroporous structures. Both of these features enable greater energy storage. Furthermore, this review presents several suggestions for meeting the challenges involved in the preparation and industrial application of electrospun porous nanofibers for advanced energy storage systems.

Introduction

Energy storage devices with high energy/power density and long cycling life, such as lithium-ion batteries (LIBs), lithium–air batteries (LABs), lithium–sulfur batteries (LSBs), sodium-ion batteries (NIBs) or supercapacitors (SCs) [1–3], are urgently needed to meet the ever-growing requirements of large-scale electric energy storage and of electric vehicles. Among the various materials suited for electrochemical energy storage, nanostructured materials with high surface-area-to-volume ratios play an increasingly important role [4]. These materials can increase the interface areas between solids and liquids or solids and gases, while at the same time shortening the diffusion distance, thereby facilitating electron or ion transport and improving electrochemical performance.

Address correspondence to E-mail: zhangjiwei@henu.edu.cn; jwzhang@henu.edu.cn

DOI 10.1007/s10853-017-0794-2

Ordinary nanoparticles, however, tend to aggregate and thereby minimize surface energy, which leads to reduction in the surface-area-to-volume ratio for nanostructured materials. One-dimensional (1D) nanomaterials, such as nanowires, nanorods, nanofibers (NFs) and nanotubes, are attracting a great deal of interest from developers of energy storage applications, as these materials have better electrical and physicochemical properties than nanoparticles [5–10]. These 1D nanomaterials can be prepared by a variety of methods, including self-assembly [11, 12], hydrothermal synthesis [13–15], template-assisted synthesis [16, 17], vapor-phase approaches [18], wet spinning [19], centrifugal spinning [20–24] or electrospinning [25–27]. Among these methods, electrospinning has special significance for the fabrication of NFs, as this technique allows facile and cost-effective fabrication of continuous, ultrathin NFs.

Electrospinning is a process that produces polymer NFs under the influence of an external electric field. This fiber production method was first proposed in [28], and it has since been widely applied for energy storage systems. As shown in Fig. 1, an electrospinning apparatus consists of a high-voltage supply, a grounded collector and a spinneret. The viscous electrospinning solution in the syringe is extruded by a feeding pump at a constant rate. Next, a high voltage is applied to the tip of the spinneret, and the solution inside the needle is charged. As the applied voltage increases, the hemispherical surface of the polymer solution is elongated to form a conical shape known as the Taylor cone. When the voltage is sufficiently high, the electrostatic forces overcome the surface tension of the liquid drop. A charged jet of the solution is then ejected from the tip of the Taylor cone and splits into many tiny jets between the tip and the collector. As the solvent evaporates, solidified continuous fibers form on the collector [29].

The morphologies and structures of electrospun NFs are greatly affected by a range of experimental parameters, such as the electric field [30], the polymer, solvent [31], nozzle [32], temperature [33] or humidity [34]. This variability of the NFs characteristics makes it feasible to properly adjust the electrospinning and to acquire electrospun NFs with various structures [35, 36]. For example, by properly selecting controllable parameters, one can fabricate porous, hollow or core–shell fibers, and fiber-in-tube or tube-in-tube structures [37, 38]. In addition, by controlling the post-treatment process (e.g., by heating as-spun NFs under different atmospheres), one can obtain various types of NFs such as metal or metal oxide NFs, carbon nanofibers (CNFs) or composite NFs [25, 39–42].

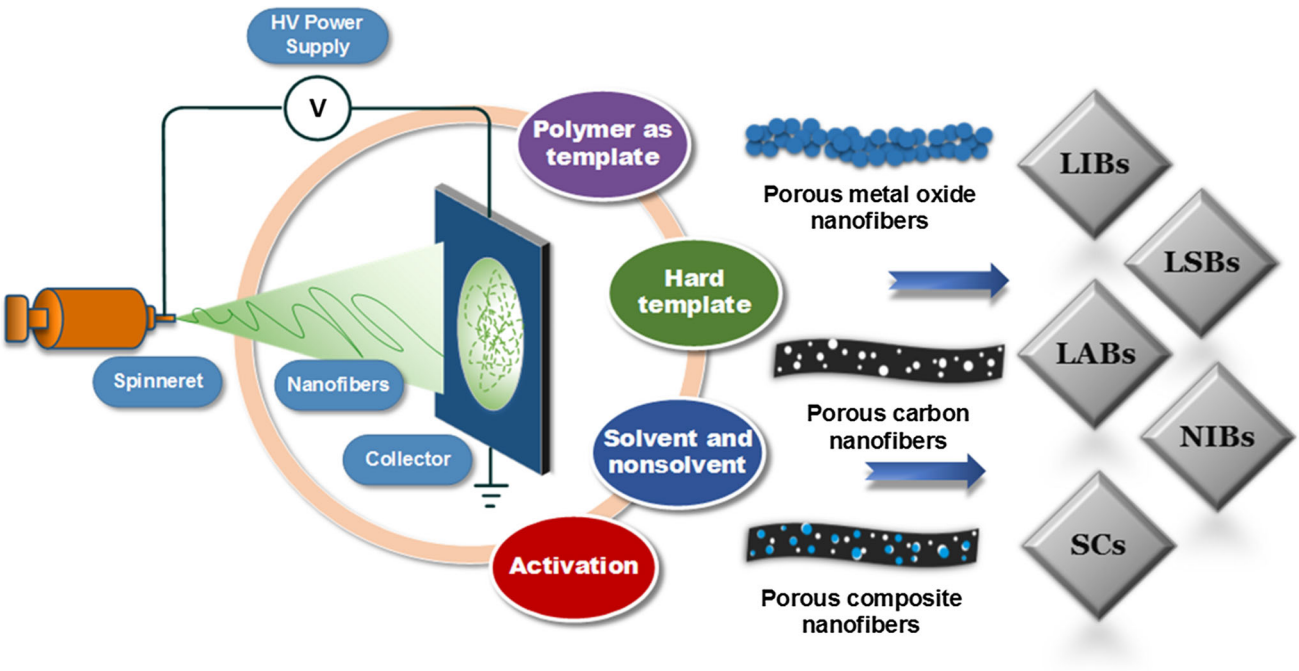

Figure 1 Schematic illustration of electrospinning apparatus and various methods applicable to preparing porous NFs for electrochemical energy storage devices.

Electrospun NFs with porous structures may find productive applications in the field of energy storage, because they exhibit high specific surface areas and abundant pore structures that can improve the transmission dynamics of electrons and ions, thereby offering enhanced performance in electrochemical energy storage. The void spaces in the porous NFs can effectively buffer changes in the volume of electrode materials during the charge and discharge processes. Due to these advantages, many methods have been established based on the electrospinning technique for preparing highly porous NFs.

The huge number of currently available publications about porous NFs provides a good opportunity to summarize the present knowledge about electrospinning techniques for preparing porous NFs and to thereby provide a reference for future studies. Therefore, in this review, we focus on several kinds of methods based on electrospinning for preparing porous NFs. An emphasis is placed on the electrospinning techniques that use polymer as the template, and on the hard template, solvent-induced, nonsolvent-induced, and activation routes. At the same time, we also summarize the potential applications of porous NFs and their composites in electrochemical energy storage systems such as LIBs, LABs, LSBs, NIBs and SCs.

Electrospinning with polymer as the template

In the electrospinning process, the polymer usually acts as the matrix of the NFs, but it can also act as a template to produce porous structures. For example, with a single polymer as the template, porous metal oxide NFs can be obtained by removing the polymer that surrounds the nanoparticles. In addition, various blended polymers with different properties can be used as templates to prepare porous carbon nanofibers (PCNFs) and composites.

Electrospinning with a single polymer template to prepare porous metal (oxide) nanofibers

With polymer/inorganic nanoparticles or corresponding precursor solutions as the starting materials for electrospinning and subsequent calcination, hierarchical porous NFs composed of numerous nanoparticles can be confined in the polymer fibers and assembled into 1D structure. The resultant porous fiber structures can be prevented from aggregating, thereby better enabling the function of the nanoparticles. The void spaces among the nanoparticles and the gaps between the fibers serve to increase the specific surface area, and they facilitate the penetration of liquid electrolytes. This permeability, along with the porous structure's capacity to buffer expansion in the volume of electrode materials during the charge/discharge process, contributes to improving the capacity for electrochemical energy storage. The single polymer template electrospinning method is mainly used to synthesize metal oxide NFs, for which the calcination process is conducted in the air atmosphere. In this process, the oxygen in the air allows complete combustion of the polymeric carbon, thereby adding to the porous structure of the as-fabricated metal oxide NFs, and enhancing energy storage.

Polyvinylpyrrolidone (PVP), with its high spinnability and good solubility in various solvents [such as *N*,*N*-dimethylformamide (DMF), water or ethanol], is often used as a template for fabricating neat metal oxide fibers. For example, Lu et al. [43, 44] prepared PVP/$SnCl_2$ NFs via electrospinning. By heating the PVP/$SnCl_2$ NFs under an air atmosphere to remove the PVP, these researchers obtained porous SnO_2 nanotubes. In addition, they found that the concentration of $SnCl_2$ had a major influence on the formation of SnO_2 nanotubes and NFs. With a low concentration of $SnCl_2$ in a PVP matrix, porous SnO_2 nanotubes could be obtained, because the scattered $SnCl_2$ molecules tended to be diffused to the surfaces of the NFs and then decomposed to form SnO_2 nanoparticles. However, if the concentration of $SnCl_2$ in the PVP matrix was high, larger number of $SnCl_2$ molecules in the fibers decomposed to form SnO_2 nanoparticles, which were uniformly distributed in the NFs.

Kundu and Liu [45] dissolved $Ni(CH_3COO)_2$, $C_6H_8O_7$, and PVP in deionized water for electrospinning, and they collected the as-spun NFs with a Ni foam. After heat treatment, porous NiO NFs were obtained and directly used in SCs without any binder. These as-fabricated SCs exhibited a capacitance retention as high as 570 F g^{-1} even at a current density of 40 A g^{-1}. The excellent performance of these SCs can be attributed to the highly porous structure of the electrodes, which facilitated the

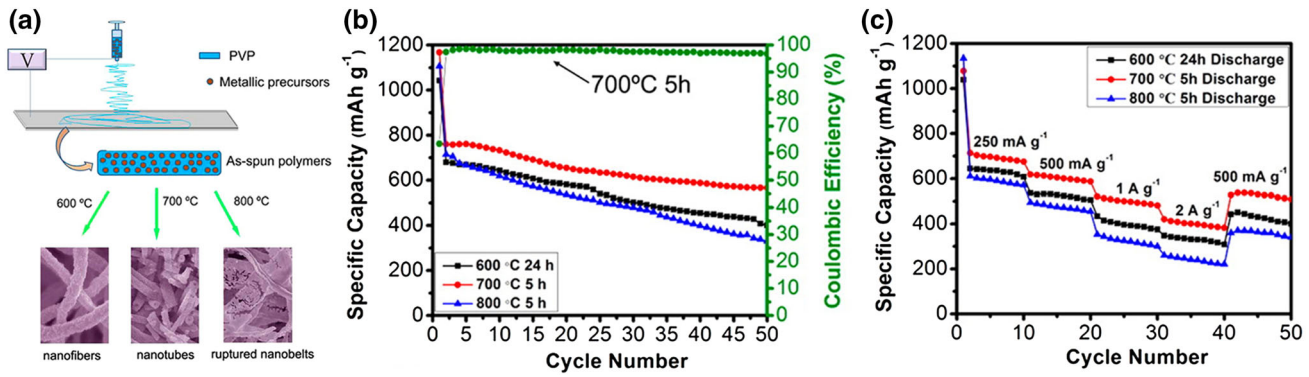

Figure 2 **a** Schematic diagram illustrating the formation process of $CaSnO_3$ nanofibers, nanotubes and ruptured nanobelts. **b** Cyclability of electrospun $CaSnO_3$ nanomaterials (current density = 60 mA g^{-1}). **c** Capacity of $CaSnO_3$ nanomaterials at different current densities. Diagrams reprinted with permission from Ref. [64]. Copyright 2012, American Chemical Society.

transport of ions and electrons. Porous NiO NFs prepared by electrospinning exhibited good electrochemical performance when applied in LIBs [46–48]. In addition, Fe_2O_3 [49], Co_3O_4 [50] and V_2O_5 [26, 51–55] NFs prepared by the same method exhibited similarly excellent electrochemical properties.

Actually, porous metal NFs can also be prepared by a single polymer template electrospinning method, because reducing the electrospun metal oxide NFs affords metallic NFs [56, 57]. With colloidal SiO_2 and poly(acrylic acid) as the starting materials, Lee et al. [56] fabricated 3D mesoporous silicon NFs by using a simple technique involving electrospinning and the magnetic-isothermic reduction in silica. The constituent Si nanoparticles formed mesoporous, interconnected nanostructures that permitted the fibers not only to accommodate large changes in volume during battery operation, but also to achieve greater access to Li^+ ions. The 3D mesoporous silicon NFs exhibited a high reversible capacity of 2846.7 mAh g^{-1} at a current density of 0.1 A g^{-1}, a stable capacity retention of 89.4% after 100 cycles at a 1 C rate (2 A g^{-1}) and a rate capacity of 1214 mAh g^{-1} even at 36 A g^{-1}.

In the presence of multicomponent precursors of metal oxides, binary metal oxide NFs, such as $ZnFe_2O_4$ [58], $ZnCo_2O_4$ [59], $ZnMn_2O_4$ [60], $NiFe_2O_4$ [61], $Li_4Ti_5O_{12}$ [62] or $LiNb_3O_8$ [63] NFs, can be fabricated as the anode materials for LIBs. For example, Li et al. [64] fabricated $CaSnO_3$ NFs and nanotubes for LIBs by using $SnCl_2$ and $Ca(NO_3)_2$ as the starting materials. They found that the morphology of as-fabricated $CaSnO_3$ was largely dependent on the calcination temperature (Fig. 2). $CaSnO_3$ nanotubes showed a better rate capability and cyclability than $CaSnO_3$ NFs or $CaSnO_3$ ruptured nanobelts. The excellent electrochemical performances of these nanotubes were attributed to their unique porous and hollow interior structures, which enabled the charge/discharge process of LIBs.

By combining a gradient electrospinning method with a controlled pyrolysis method, Niu et al. [65] synthesized various mesoporous metal oxide nanotubes as cathode materials for LIBs and NIBs. Moreover, electrospinning could also be adopted to prepare porous $CuCo_2O_4$ [66] NFs and $ZnCo_2O_4$ [67] nanotubes used in SCs. Table 1 shows the electrochemical performances for several kinds of metal oxide NFs used in LIBs.

Electrospinning can also be combined with calcination to deposit a carbon coating layer on porous metal oxide NFs, thereby significantly improving their electrochemical performance. Zhu et al. [68] prepared porous α-Fe_2O_3 NFs by electrospinning. Then, they dispersed the porous α-Fe_2O_3 NFs into PVP and calcined the mixture under a nitrogen atmosphere to obtain α-Fe_2O_3/C NFs. The as-obtained α-Fe_2O_3/C NFs exhibited a high reversible capacity of 842 mAh g^{-1} after 50 cycles of charge/discharge at a current density of 50 mA g^{-1}.

Xu et al. [69] added the precursor of $Li_4Ti_5O_{12}$ (LTO) to an ethanol solution of PVP and obtained composite fibers by electrospinning. They further calcined the as-spun composite fibers in an Ar/H_2 atmosphere to obtain LTO/C fibers. After being heated in air, the resultant LTO/C fibers were transformed into porous LTO/C (PLTO/C) composite NFs, which exhibited a

Table 1 Porous metal oxide nanofibers for LIBs

Material	Electrospinning solution (precursor/polymer/solvent)	Electrochemical performance	References
SnO_2 nanofibers	$SnCl_2$/PVP/DMF	597 mAh g^{-1} after 300 cycles at 160 mA g^{-1}	[70]
SnO_2 nanotubes	$SnCl_4$/PVP/Et (Et = ethanol)	807 mAh g^{-1} after 50 cycles at 180 mA g^{-1}	[71]
SnO_2 nanofibers	$SnCl_2$/PVP/DMF, Et	320 mAh g^{-1} after 20 cycles at 156 mA g^{-1}	[72]
GeO_2/SnO_2 nanofibers	$SnCl_2$, GeO_2/PVP/DMF, Et	680 mAh g^{-1} after 50 cycles	[73]
SnO_2 nanotubes	$SnCl_2$, mineral oil/PVP/DMF, Et	645 mAh g^{-1} after 50 cycles at 100 mA g^{-1}	[44]
SnO_2/ZnO nanotubes	$SnCl_2$, $Zn(NO_3)_2$/PVP/DMF, Et	585 mAh g^{-1} after 45 cycles at 168 mA g^{-1}	[74]
$CaSnO_3$ nanotubes	$SnCl_2$, $Ca(NO_3)_2$/PVP/Et, DMF	565 mAh g^{-1} after 50 cycles at 60 mA g^{-1}	[64]
NiO nanofibers	$Ni(NO_3)_2$/polyacrylonitrile (PAN)/DMF	638 mAh g^{-1} after 50 cycles at 40 mA g^{-1}	[46]
NiO nanofibers	$Ni(Ac)_2$/PVAc/DMF (Ac = acetic acid)	583 mAh g^{-1} after 100 cycles at 80 mA g^{-1}	[47]
NiO/ZnO nanofibers	$Ni(NO_3)_2$, $Zn(NO_3)_2$/PVP/ethanol, water	949 mAh g^{-1} after 120 cycles at 200 mA g^{-1}	[48]
Fe_2O_3 nanotubes	$Fe(AcAc)_3$/PVP/DMF	987 mAh g^{-1} after 200 cycles at 200 mA g^{-1}	[49]
a-Fe_2O_3/C nanofibers	$Fe(Ac)_2$/PVP/Et, water	842 mAh g^{-1} after 50 cycles at 50 mA g^{-1}	[68]
Co_3O_4 nanotubes	$Co(Ac)_2$/PVP/DMF	1826 mAh g^{-1} after 100 cycles at 300 mA g^{-1}	[50]
$ZnFe_2O_4$ nanofibers	$Zn(CH_3COO)_2$, $Fe(NO_3)_3$/PVP/Et	733 mAh g^{-1} after 30 cycles at 60 mA g^{-1}	[58]
$ZnCo_2O_4$ nanotubes	$Zn(NO_3)_2$, $Co(NO_3)_2$/PVP/Et, Ac, water	1454 mAh g^{-1} after 30 cycles at 100 mA g^{-1}	[59]
$ZnMn_2O_4$ nanofibers	$Zn(Ac)_2$/PVP/methyl alcohol, Ac	658 mAh g^{-1} after 100 cycles at 400 mA g^{-1}	[60]
$NiFe_2O_4$ nanofibers	$Fe(AcAc)_3$, $Ni(Ac)_2$/PVP/Et	1000 mAh g^{-1} after 300 cycles at 20 C	[61]
$Li_4Ti_5O_{12}$ nanofibers	Tetrabutyl titanate, lithium acetate/PVP/Et, Ac	120 mAh g^{-1} after 100 cycles at 400 mA g^{-1}	[62]
$Li_4Ti_5O_{12}$/C nanofibers	Lithium acetylacetonate, titanium isopropoxide/PVP/Et, Ac	131.6 mAh g^{-1} after 100 cycles at 20 C	[69]
$LiNb_3O_8$ nanofibers	Lithium acetylacetonate, $Nb(OC_2H_5)_5$/PVP/Et, Ac	92.7 mAh g^{-1} after 1000 cycles at 1 C	[63]
$LiMn_2O_4$ nanofibers	$LiNO_3$, $Mn(Ac)_2$/PVP/ethanol, Ac	87% of capacity retained after 1250 cycles at 1 C	[75]
$LiNi_{0.4}Mn_{1.6}O_4$ nanofibers	Lithium acetate, $C_4H_6NiO_4$, $C_4H_6MnO_4$/PVP/Et, water	91% of capacity retained after 100 cycles at 1 C	[76]

high specific capacity of 143 mAh g^{-1} even at a high rate of 30 C. Furthermore, the PLTO/C composite NFs were applicable for asymmetric hybrid SCs.

These studies demonstrated that the introduction of a carbon coating on the surfaces of porous metal oxide NFs serves to greatly improve the conductivity. Meanwhile, the carbon shell can limit the growth of crystallite in heating process and effectively buffer the volume expansion of the anode materials during the charge/discharge processes.

LABs show promising potential as energy storage devices because they exhibit a very high theoretical energy density, and their metal oxides can act as catalysts to facilitate the oxygen reduction reaction and promote oxygen evolution. Li et al. [77] dissolved $La(NO_3)_3$, $Sr(NO_3)_2$, $Co(CH_3COO)_2$ and PVP in DMF and obtained a homogeneous viscous solution for electrospinning. The as-prepared electrospun NFs were transformed into porous $La_{0.5}Sr_{0.5}CoO_{2.91}$ NFs after being calcined in air. Thanks to their porous structures, the as-fabricated $La_{0.5}Sr_{0.5}CoO_{2.91}$ NFs exhibited an initial discharge capacity of 7205 mAh g^{-1}, at a current density of 100 mA g^{-1} (the voltage platform being around 2.66 V). In addition, Li et al. [78] synthesized porous $NiCo_2O_4$ nanotubes for LABs by electrospinning and acquired excellent cycling stability over 110 cycles of charge/discharge.

In these studies, the authors drew a common conclusion that hierarchical porous structures can provide channels for electron and oxygen transport, and such structures can also provide a large contact area of electrode–electrolytes to ensure a highly efficient catalytic reaction, thereby significantly improving the electrochemical performance of LABs.

Electrospinning with a polymer blend as the template

Polymers with different physical and chemical properties can be blended to compose templates for

fabricating porous carbon NFs and composite NFs by electrospinning. This approach is the so-called polymer blend template electrospinning method. The polymer blend consists of two types of polymers with different degrees of thermal stability. The polymer with less thermal stability undergoes pyrolysis upon thermal decomposition, which creates pores in the carbon matrix. These pores are formed through the carbonization of the thermally stable polymer. The size and structure of the pores can be controlled by manipulating the thermal stability and compatibility (or solubility) of the various polymers, and greater differences in their compatibility lead to larger sized pores [79]. Table 2 lists a variety of the PCNFs that can be prepared via polymer blend template electrospinning method.

To obtain porous carbon NFs through the polymer blend template electrospinning method, researchers often blend polyacrylonitrile (or PAN, a common carbonizing polymer) with other polymers such as polymethyl methacrylate (PMMA) [80–86] or polystyrene (PS) [87–90]. As PAN exhibits poor compatibility with PMMA (the sacrificial phase), island-like PMMA is formed in the PAN matrix when the PAN/PMMA solution undergoes electrospinning. During calcination in an inert atmosphere, the PAN NFs are carbonized to afford a carbon matrix, and PMMA is completely pyrolyzed to form pores in the carbon NFs.

Usually, PAN acts as the continuous phase in the PAN/PMMA NFs, and PMMA acts as the dispersed phase. However, Wei et al. [81] combined the electrospinning of a PAN/PMMA solution (consisting of PAN as the dispersed phase and PMMA as the continuous phase, and having a PAN/PMMA molar ratio of 3:7) with a calcination process, to prepare highly flexible PCNFs. When these as-fabricated, highly flexible PCNFs were used as the electrode materials for SCs, they could deliver a specific capacitance of 86 F g^{-1}.

Peng and Lo [82] formulated PAN/PMMA solutions with differing compositions for electrospun and fabricated PCNFs. When directly used as an LIB anode without any binder, those PCNFs (prepared at a PAN/PMMA molar ratio of 5:5) exhibited greatly increased porosity and a high discharge capacity of 446 mAh g^{-1} under a current density of 150 mA g^{-1}, with a favorable cycle stability (discharge capacity 354 mAh g^{-1}) after 100 cycles at a current density of 200 mA g^{-1} (Fig. 3).

Table 2 Various PCNFs prepared via the polymer blend template electrospinning method

Purpose	Precursor and additives/solvent	Specific surface area (m^2 g^{-1})	Electrochemical performance	References
LIBs	PAN, PMMA/DMF	572.9	231.8 mAh g^{-1} after 20 cycles at 50 mA g^{-1}	[80]
EDLCs	PAN, PMMA and graphene/DMF	1051.65	~120 F g^{-1} after 100 cycles at 20 mA cm^{-2}	[84]
Structure	PAN, PMMA/DMF	940	–	[83]
EDLCs	PAN, PMMA (different molecular weight)/DMF	248	210 F g^{-1} at 2 mV s^{-1}	[85]
LIBs	PAN, PMMA/DMF	306	354 mAh g^{-1} after 100 cycles at 200 mA g^{-1}	[82]
EDLCs	PAN, PMMA and TEOS/DMF	699	170 F g^{-1} after 8000 cycles at 1 A g^{-1}	[86]
EDLCs	PAN, PMMA/DMF	467.57	86 F g^{-1} at 5 mV s^{-1}	[81]
Zn–air batteries	PAN, PS/DMF	1271.2	Peak power density is 194 mW cm^{-1} (0–340 mA·cm^{-2})	[87]
EDLCs	PAN, PS/DMF	535	262 F g^{-1} at 200 mA g^{-1}	[89]
EDLCs	PAN, PS/DMF	750	270 F g^{-1} at 0.5 A g^{-1}	[90]
LIBs	PAN, PLLA/DMF	235	435 mAh g^{-1} after 50 cycles at 50 mA g^{-1}	[91]
Properties	PVDF, PEO/DMF	382.3	–	[92]
EDLCs	PAN, Nafion/DMF	1614	210 F g^{-1} at 1 A g^{-1}	[93]
NIBs	PAN, F127/DMF	178.69	266 mAh g^{-1} after 100 cycles at 50 mA g^{-1}	[94]
EDLCs	PAN, PEG–PSO–PEG/DMF	656	289 F g^{-1} at 0.2 A g^{-1}	[95]
EDLCs	PAN, PPS/DMF	718.1	130 F g^{-1} at 20 mA cm^{-2}	[96]
EDLCs	PAN, PMHS/DMF	302.5	126.86 F g^{-1} at 1 mA cm^{-2}	[97]
Structures	PAN, PVP/DMF	571.47	–	[98]
LIBs	PAN, SAN/DMF	13	391 mAh g^{-1} after 10 cycles at 200 mA g^{-1}	[99]

Kim et al. [84] reported that graphene could increase the electrical conductivity and specific surface area of PCNFs prepared by the electrospinning of PAN/PMMA. The resultant graphene-doped PCNFs exhibited a much higher specific capacitance (128 F g^{-1}) than the undoped PCNFs. As reported elsewhere, these researchers also considered that the superior electrochemical performance of PAN/PMMA-derived carbon NFs could be attributed to their hierarchical pores and their high specific surface areas, which provided favorable contact between the electrodes and electrolytes and facilitated the transport of electrolyte ions.

PS [87, 89, 90], poly-L-lactic acid (PLLA) [91], poly(ethylene oxide) [92], Nafion [93], F127 [94], polyethylene glycol–polysiloxane–polyethylene glycol [95], polyphenylsilane [96] and polymethylhydrosiloxane [97] can also be used as the sacrificial templates for preparing PCNFs. Zhang et al. [98] formulated PAN/PVP solutions with differing molar ratios and obtained porous PAN NFs by electrospinning in association with follow-up treatment in water to remove PVP. The pore sizes and pore distributions of the porous PAN NFs could be easily controlled by varying the content of PVP in the composite polymer precursor. Also, the porous PAN NFs obtained at a PAN/PVP molar ratio of 0.8:1 could be carbonized in N_2 atmosphere to form PCNFs with a specific surface area of 571.47 m^2 g^{-1}.

Using styrene-*co*-acrylonitrile (SAN)/DMF core/emulsified PAN-SAN/DMF shell solution as a precursor, Lee et al. [99] prepared porous hollow carbon nanofibers (pHCNFs) by coaxial electrospinning. During heat treatment, the SAN was burnt out, and the PAN was carbonized to form PCNFs (Fig. 4). The researchers found that the spacing between the graphene layers in the pHCNFs increased, owing to the hundred layer-sequential mismatches which occurred through pores by formation. This expanded structure promoted lithium-ion insertion and extraction. The resultant PCNFs, when used as the anode materials of LIBs, exhibited a high initial capacity of 1003 mAh g^{-1} at a current density of 50 mA g^{-1}.

In addition to neat PCNFs, PCNFs containing inorganic nanoparticles can also be prepared by mixing polymer blends and the precursors of inorganic nanoparticles for electrospinning. For example, by combining the PAN/PMMA polymer blend template with the precursor of inorganic nanoparticles, one can conduct electrospinning to obtain inorganic nanoparticles coated by PCNFs. The resultant PCNF-coated inorganic nanoparticles, such as SnSb [100, 101], TiO_2 [102, 103], RuO_2 [104, 105], Si [106, 107], P [108] or Sn [109, 110], exhibit good long-

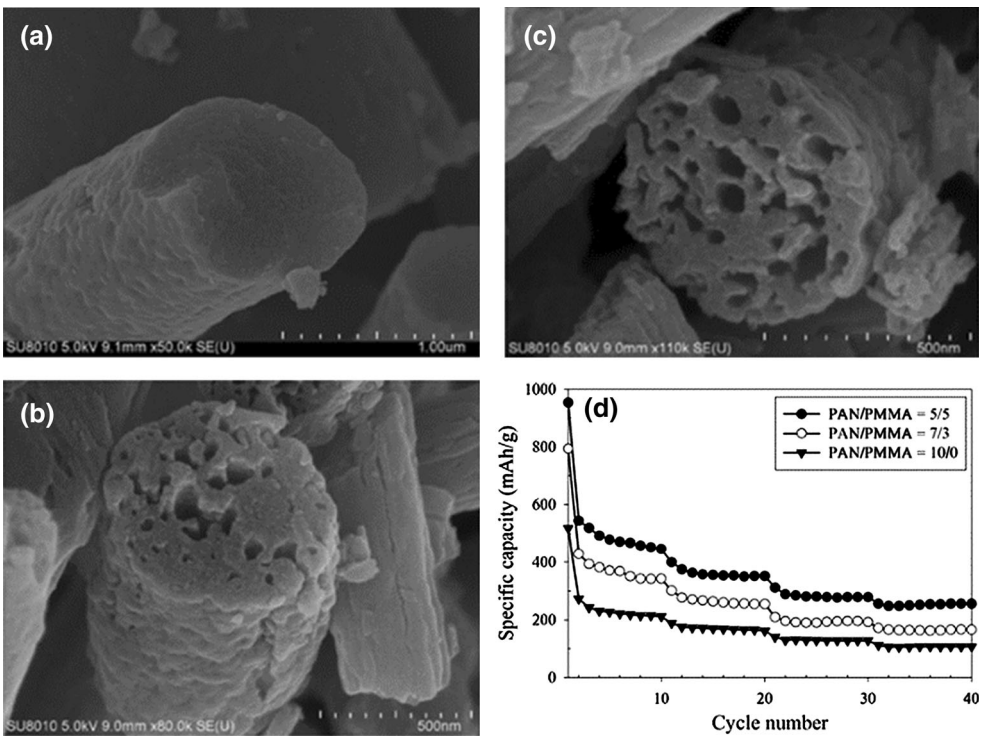

Figure 3 SEM micrographs of carbonized electrospun fibers of **a** PAN/PMMA = 10:0; **b** PAN/PMMA = 7:3; **c** PAN/PMMA = 5:5; and **d** their rate capacities at different current densities when used as anodes for LIBs. Images reproduced from Ref. [82], with permission of Springer.

term cyclic stability and high rate capability in energy storage devices, because the PCNFs derived from PAN/PMMA can effectively buffer the large volume changes during the cyclic process and thereby improve the conductivity.

Yu et al. [109] conducted electrospinning of PMMA–PAN–tin octoate in DMF solution. By heating the resultant PAN-coated tin octoate in air at 250 °C, they obtained PAN-coated SnO_2 nanoparticles. The carbonization of these PAN-coated SnO_2 nanoparticles under an Ar/H_2 atmosphere afforded multichannel PCNFs with Sn nanoparticles (Fig. 5). The as-fabricated multichannel PCNFs with Sn nanoparticles, when used as the anode material for LIBs, exhibited a reversible discharge capacity as high as 648 mAh g^{-1} even after 140 cycles. With PLLA [111, 112] and F127 [113] as the sacrificial polymer templates, PCNFs/Si nanoparticles could be prepared as the composite anode material for LIBs.

In a similarly way, Qin et al. [88] added Fe_3O_4 nanoparticles to a PAN/PS solution for electrospinning and obtained Fe_3O_4/PCNFs by calcination. The porous carbon framework was able not only to buffer the volume expansion of Fe_3O_4 and to facilitate transfer of electrons and ions, but also to accelerate the formation of a stable SEI film outside the composite, thereby preventing the electrolyte from contacting the Fe_3O_4 directly. The as-fabricated Fe_3O_4/PCNFs exhibited a reversible capacity of 596 mAh g^{-1} at 2.0 A g^{-1} and a slow fade in capacity after 200 cycles of charge/discharge (541 mAh g^{-1}).

It is widely accepted that using PCNF as the shell can prevent the volumetric expansion of metal (oxide) during the charge/discharge processes, and it can improve the electrical conductivity (as the channels of PCNFs allow for rapid transport of ions and electrons). More importantly, the pore sizes and structures of PCNFs can be easily controlled by adjusting the compositions and proportions of the polymer blends. Therefore, it is important to screen suitable solvents and formulate stable solutions of the polymer blends for electrospinning as a means to fabricate PCNFs with excellent electrochemical performance.

In the process of electrospinning with a polymer blend, one polymer is used as the template inside another polymer to form holes after heating. The sacrificial polymer acts as the pore-making template to form pores in the NFs. Meanwhile, the pore formation can be adjusted by manipulating the polymer compatibility in the polymer blend [79].

Hard template method based on electrospinning

Nanoparticles can be used as the hard templates to prepare porous carbon materials. The inorganic nanoparticles, added as hard templates in the polymer precursors for electrospinning, can be removed by corrosive acids or alkalis to afford uniform pores in the NFs. The pore diameter can be controlled by adjusting the size of the nanoparticles.

Table 3 lists a series of PCNFs prepared by hard template electrospinning, in which metals or metal oxides, such as SiO_2 [86, 114–117], Sn [118, 119], ZnO [120, 121], Zn [122], Fe [123] or Ni [114, 124, 125], are presented as the materials most commonly used as hard templates for preparing electrospun PCNFs.

Ji et al. [115] directly added SiO_2 nanoparticles into a PAN/DMF solution for electrospinning. They conducted carbonization of the electrospun PAN/SiO_2 composite NFs in a nitrogen atmosphere, followed by immersion in an HF acidic solution to remove the SiO_2. The resultant PCNFs had an

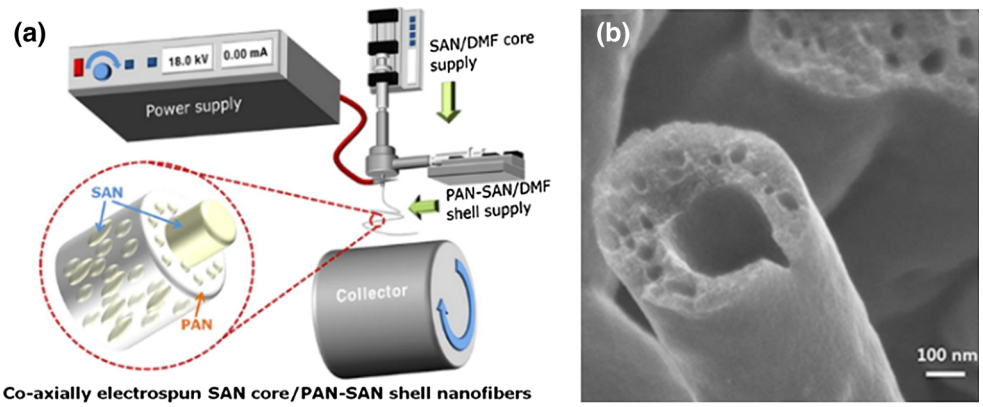

Figure 4 **a** Schematic diagram illustrating the electrospinning process of SAN core/PAN-SAN shell nanofibers. **b** FE-SEM images of porous hollow carbon nanofibers. Images reprinted with permission from Ref. [99]. Copyright 2012, American Chemical Society.

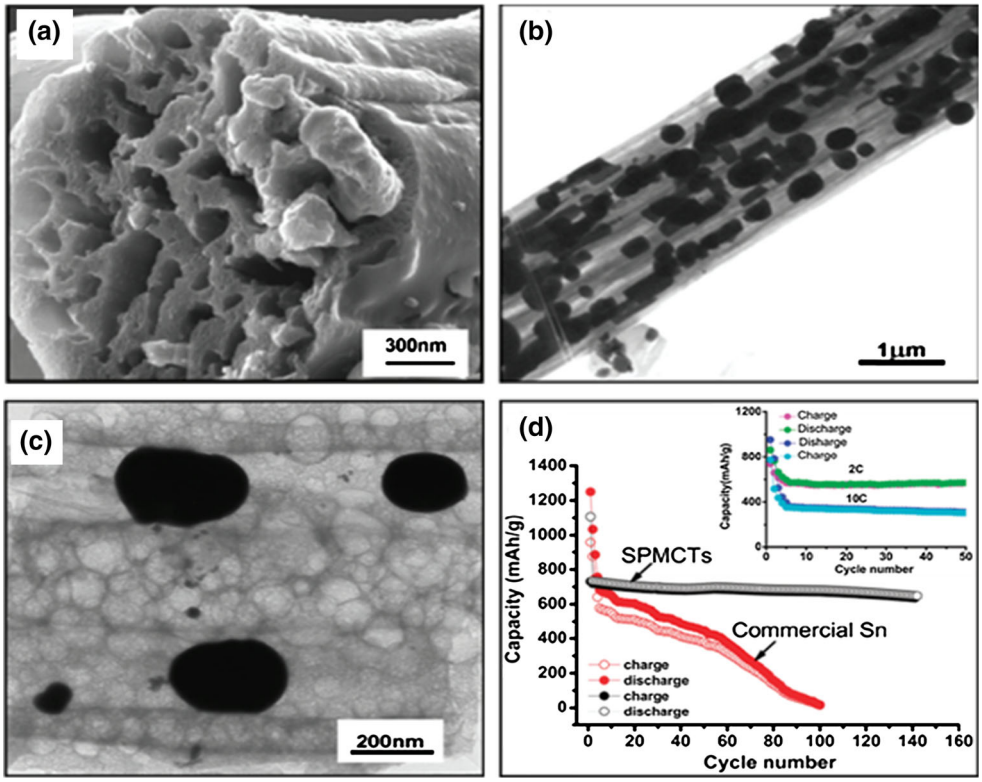

Figure 5 **a** Cross-sectional images and **b**, **c** TEM micrographs of Sn encapsulated in porous multichannel carbon nanofibers (SPMCTs); **d** cyclability of SPMCTs and commercial Sn nanopowders with similar sizes (~200 nm) at a cycling rate of 0.5 C (current density 100 mA g^{-1}). *Note* the *inset* displays the discharge capacity of the SPMCTs electrodes as a function of the discharge rate at 2 and 10 C. Images reprinted with permission from Ref. [109]. Copyright 2009, American Chemical Society.

increased specific surface area and an improved capacity as anode material for LIBs. Nan et al. [116] used tetraethoxysilane (TEOS) and polyamic acid (PAA) to fabricate electrospun NFs. In the process of carbonization, the TEOS decomposed to form SiO_2, which was homogeneously dispersed in the carbon NFs. After etching with HF acid, the SiO_2 nanoparticles were eliminated, and a PCNF fabric with a large specific surface area (950 m^2 g^{-1}) and a reversible capacity of 445 mAh g^{-1} (at the 50th cycle under 50 mA g^{-1}) was obtained.

Some metal nanoparticles can act not only as the hard template, but also as the catalyst to promote the graphitization of PCNFs. Zhang et al. [123] prepared PAN fibers containing numerous Fe particles by electrospinning. The carbonization of the resultant Fe-doped PAN fibers in N_2 atmosphere and the etching of the carbonized PAN fibers with an HNO_3 solution afforded PCNFs in which the Fe nanoparticles not only served as a sacrificial phase for the production of pores, but also acted as the catalyst to promote the graphitization of the carbon NFs. Moreover, etching with HNO_3 could introduce oxygenated groups that acted as the active sites for Li-ion storage. As a result, the as-prepared PCNFs exhibited an exceptionally high capacity of 983 mAh g^{-1} at a current density of 100 mA g^{-1}.

Chen et al. [125] conducted coaxial electrospinning of a PAN/nickel acetate ($Ni(Ac)_2$)/PMMA composite solution and obtained carbon nanotube/carbon nanofiber hybrid material in which $Ni(Ac)_2$ was decomposed to form Ni nanoparticles and PMMA was decomposed to produce pores during calcination (Fig. 6). After activation, the final carbon nanotube/carbon nanofiber hybrid material exhibits a high specific surface area (1840 m^2 g^{-1}). This characteristic was achieved because the Ni nanoparticles could be removed to produce pores, and the Ni could act as a catalyst to enhance the growth of carbon nanotubes. When the as-prepared hybrid material was applied as the anode for LIBs, it exhibited a reversible capacity of ~1150 mAh g^{-1} after 70 cycles at a current density of 0.1 A g^{-1}, and a capacity retention of more than 80% after 3500 cycles of charge/discharge at a current density of 8 A g^{-1}.

Certain varieties of inorganic salts such as sodium dodecyl sulfate (SDS) [126], $CaCO_3$ [127] or $NaHCO_3$ [128] can also be used as hard templates for preparing PCNFs by electrospinning. Nagamine et al. [126]

Table 3 A series of PCNFs prepared via the hard template method

Purpose	Precursor/template/solvent	Specific surface area ($m^2\ g^{-1}$)	Electrochemical performance	References
EDLCs	PAN, PMMA/SiO_2/DMF	699	170 F g^{-1} after 8000 cycles at 1 A g^{-1}	[86]
EDLCs	P123, PVP, PF/SiO_2, Ni/ethanol	1790	303 F g^{-1} at 0.7 A g^{-1}	[114]
LIBs	PAN/SiO_2/DMF	91.8	454 mAh g^{-1} after 10 cycles at 50 mA g^{-1}	[115]
LIBs	PAA/SiO_2/DMAc	950	445 mAh g^{-1} after 50 cycles at 50 mA g^{-1}	[116]
Properties	F127, PVP, PF/SiO_2/ethanol	1642	–	[117]
EDLCs	PAN, PVP/Sn/DMF	1082	289 F g^{-1} at 10 mV s^{-1}	[118]
EDLCs	PVA/Sn/citric acid	800	105 F g^{-1} at 5 mV s^{-1}	[119]
EDLCs	PAN/ZnO/DMF	132.70	417 F g^{-1} at 0.5 A g^{-1}	[120]
EDLCs	PAN/ZnO/DMF	413	275 F g^{-1} at 1 A g^{-1}	[121]
LIBs	PAN/Zn/DMF	438	385 mAh g^{-1} after 10 cycles at 100 mA g^{-1}	[122]
LIBs	PAN/Fe/DMF	198	609 mAh g^{-1} after 100 cycles at 1000 mA g^{-1}	[123]
LIBs	PAN, PVP/Ni/DMF	–	~330 mAh g^{-1} after 650 cycles at 3.7 A g^{-1}	[124]
LIBs	PAN, PMMA/Ni/DMF	1840	~1150 mAh g^{-1} after 70 cycles at 0.1 A g^{-1}	[125]
EDLCs	PVA/SDS/water	900	125 F g^{-1} at 5 mV s^{-1}	[126]
EDLCs	PAN/$CaCO_3$/DMF, tetrahydrofuran (THF)	679	251 F g^{-1} at 0.5 A g^{-1}	[127]
Properties	PAN/$NaHCO_3$/DMF	724	–	[128]
EDLCs	PAN g-C_3N_4/DMF	554	220 F g^{-1} at 0.2 A g^{-1}	[129]

fabricated PCNFs from a PVA solution containing diammonium hydrogen phosphate (DAP) and SDS by electrospinning. During stabilization and carbonization, the DAP and SDS were decomposed to form salt particles, which served as the templates, and these templates could be removed by leaching with water to create spherical pores.

Similarly, some organics can act as the templates to prepare PCNFs, and in some way, these templates can work better than inorganic salts, as organics can be easily removed during carbonization. Using g-C_3N_4 nanosheets as both the sacrificial template and the N-doping source, Liang et al. [129] prepared N-enriched mesoporous carbon nanofibers (NMCNFs). After the g-C_3N_4 nanosheets were totally removed during calcination to leave mesopores, the resultant NMCNFs film served as the electrode for an SC which exhibited a high specific capacitance of 220 F g^{-1} at a current density of 0.2 A g^{-1}.

It should be emphasized that any metals or metal oxides used as the templates for preparing porous carbon fibers via the electrospinning need to be removed with acids. However, the inorganic salts and organics used as the sacrificial templates can be easily removed with water or by calcination. Therefore, using inorganic salts and organics as the

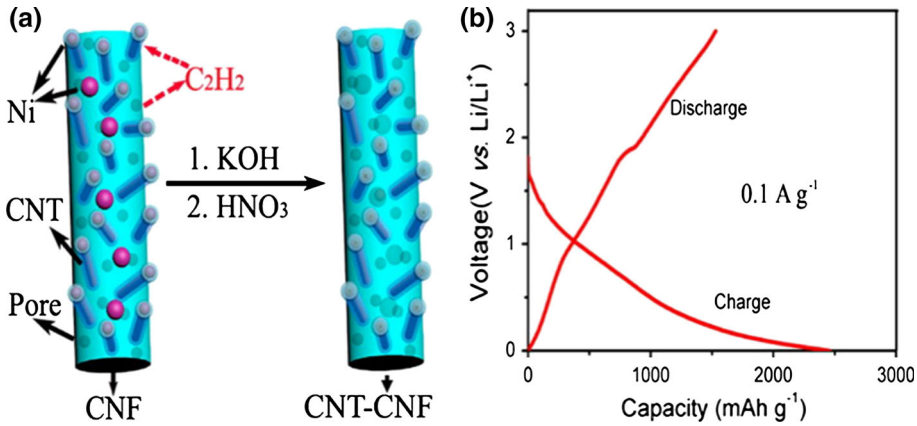

Figure 6 **a** Schematic diagram showing the design of an activated hollow carbon nanotube/carbon nanofiber hybrid material and **b** its charge–discharge voltage profiles as the anode for LIBs. Images reprinted with permission from Ref. [125]. Copyright 2013, American Chemical Society.

sacrificial templates enable better environmental acceptance, cost-effectiveness and greater prospects of application than using metals and metal oxides as the templates.

In addition to PCNFs, porous composite NFs can also be prepared through the hard template method. For example, silicon- and tin-based materials are considered promising candidates as anode materials for LIBs, because they have a high theoretical capacity. However, these materials undergo large changes in volume during charge/discharge processes, which result in the pulverization of the particles and electrical disconnection with the current collector, causing poor cyclability. Therefore, it is important to combine the Si- and Sn-based materials with PCNFs that are prepared by electrospinning and contain massive pores, because the porous PCNFs can provide void spaces to cushion the volume variation of the anode materials during the cyclic process.

In this respect, the studies conducted by several groups of researchers from China are worth special attention. To describe a few of these studies, Zhou et al. [130] calcined Si nanoparticles in air and obtained a layer of SiO_x on the surface of Si. They added the as-obtained Si@SiO_x nanoparticles into a PAN/DMF solution for electrospinning and finally obtained Si@PCNFs after carbonization in association with HF etching. The as-prepared Si@PCNFs, when used as the anode material for LIBs, maintained a reversible capacity of 1104 mAh g^{-1} after 100 cycles at 0.5 A g^{-1}, thereby showing excellent cycling performance.

Wang et al. [131] formulated a mixed solution of PVP, $SnCl_2$ and TEOS in DMF and obtained hybrid NFs by electrospinning. The resultant NFs were annealed in air at 350 °C to create SiO_x and SnO_2, and the PVP was slightly carbonized. After the SiO_x was etched with an HF solution, SnO_2/C porous NFs were obtained. SnO_2/PCNFs and Sn/PCNFs were finally obtained after SnO_2/C porous NFs were calcined in an N_2 atmosphere at 500 and 800 °C, respectively. Due to the small size of the SnO_2 nanoparticles, the as-prepared SnO_2/PCNFs exhibited a high reversible lithium storage capacity at a low current density. The Sn/PCNFs also exhibited good cycle performance at a high current density, due to the good conductivity of Sn.

Zou et al. [132] used ice as the hard template and prepared PCNFs with Sn/SnO_x nanoparticles encapsulated in their pores as LIB anode materials. As the void spaces around the Sn/SnO_2 nanoparticles were able to buffer the volumetric changes in Sn during cyclic process, the as-prepared PCNFs-Sn/SnO_x exhibited a specific capacity of 510 mAh g^{-1} after 40 cycles of charge/discharge, at a current density of 30 mA g^{-1}.

Zhou et al. [133] fabricated PCNFs with PVP as the carbon source, with F127 and SiO_2 as the sacrificial templates. By immersing the PCNF substrate into a neutral $KMnO_4$ solution, they obtained freestanding MnO_2/PCNFs with an ultrahigh surface area (1814 m g^{-1}). As a flexible electrode in an SC, the MnO_2/PCNFs exhibited a high specific capacitance of 520 F g^{-1} at 0.5 A g^{-1} and showed superior cycling stability (92.3% of the capacitance was maintained after 4000 cycles of charge/discharge).

McCormac et al. [134] prepared porous Si/TiO_2 composite NFs for LIBs by a sulfur-templating method. The porous TiO_2 NFs acted as the lithium storage materials, and these NFs could therefore efficiently compensate for the expansions in volume of Si nanoparticles during the charge/discharge processes. The porous Si/TiO_2 NFs exhibited an initial capacity of 839 mAh g^{-1} and a capacity retention of 50% after 180 cycles of charge/discharge (the specific capacity of Si NFs was reduced to 17 mAh g^{-1} after 100 cycles of charge/discharge).

It is generally recognized that in porous carbon hybrid NFs, PCNFs can provide a sufficient void space to buffer the volumetric expansion of the anode materials and thereby prevent the pulverization of the electrodes. Also, the hierarchical porous structure of the PCNFs facilitates the conductivity of the electrolyte and the lithium-ion diffusion. The size and morphology of the pores can be handily controlled by selecting the proper nanoparticles as the templates. Unfortunately, the hard template method is expensive and environmentally unfriendly, because it requires the use of acid and involves post-treatment.

Solvent- and nonsolvent-induced methods based on electrospinning

Solvent-induced method based on electrospinning

The solvent-induced method is another method that is applicable for preparing porous fibers, and it allows rapid phase separation in the volatile solvents

during the electrospinning process. The solvent-rich phase is transformed into pores, and the polymer-rich phase is solidified into the matrix through flash evaporation of the solvent, resulting in the formation of pores on the fiber surfaces [135–141]. The porous structure of the resultant NFs can be adjusted by choosing different volatile solvents.

Lin et al. [136] dissolved PS in a THF/DMF mixed solvent and formulated an electrospinning precursor solution. By varying the weight ratio of THF/DMF, they obtained final fibers with differing microporous morphologies (Fig. 7). Li et al. [138] systematically studied the influence of various solvents (dichloromethane (DCM), acetone, chloroform, THF, ethyl acetate and DMF) on the structure of electrospun PMMA fibers. They found that dense cycloidal nanopores were distributed on the surface of fibers obtained from PMMA/DCM and PMMA/ethyl acetate solutions, but elliptical nanopores formed on the fibers produced from PMMA/chloroform and PMMA/DMF/DCM solutions. Huang et al. [142] dissolved PAN in a mixed DMF/chloroform solvent for electrospinning. They then collected the electrospun fibers with a glass dish filled with ice water and obtained PCNFs after carbonization. The as-prepared PCNFs, when used as the anode material for an LSB, delivered a high reversible discharge capacity of 340 mAh g^{-1} after 100 cycles.

Nonsolvent-induced method based on electrospinning

The construction of electrospun NFs is affected by various parameters, one of them being ambient humidity, which not only affects the spinnability of the precursor but also influences the hierarchical structure of the NFs [33, 34]. Casper et al. [141] used PS/THF solution for electrospinning and found that dense pores were gradually formed on the surface of the fibers with the increase in ambient humidity. These researchers suggested that the formation of such pores could be explained by the concept of breath figures. In other words, as the solvent evaporated, the surface of the fibers cooled, and water from the air condensed on the surface of the fibers. After the liquid was evaporated completely, and the water droplets were eliminated, leaving uniformly distributed dense pores.

Kongkhlang et al. [143] prepared polyoxymethylene (POM) NFs using a hexafluoroisopropanol (HFIP)-based solvent. The as-obtained POM NFs had a nanoporous structure at 55 and 75% relative humidity. These researchers suggested that

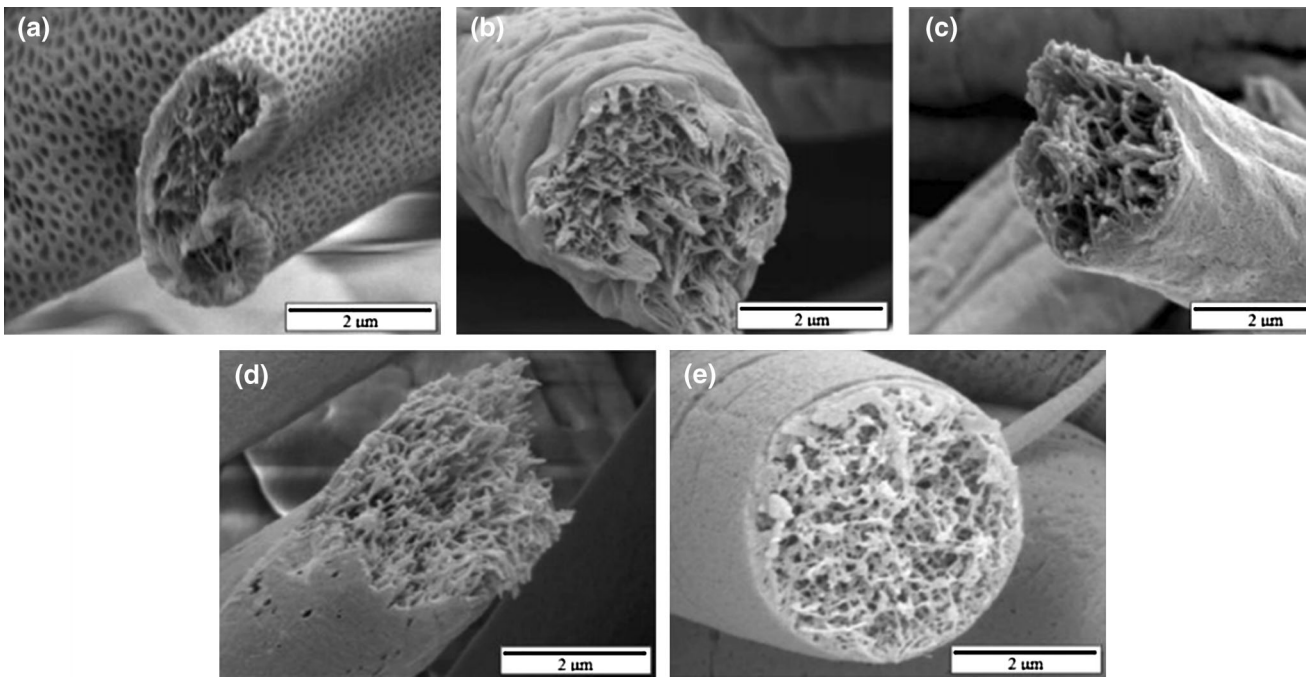

Figure 7 Cross-sectional FE-SEM images of PS fibers electrospun from 20 wt% PS solutions with different weight ratios of THF/DMF: **a** 4/0, **b** 3/1, **c** 2/2, **d** 1/3 and **e** 0/4. Images reprinted with permission from Ref. [136]. Copyright 2010, American Chemical Society.

the formation of the nanopores might be based on vapor-induced phase separation. In the electrospinning process, the HFIP rapidly evaporated, and the moisture (acting as a nonsolvent) penetrated into the fiber, resulting in phase separation. Finally, the solvent-rich phase formed the pores, and the polymer-rich phase formed the matrix.

Fashandi et al. [144] prepared PS/DMF and PS/THF solutions for electrospinning at different levels of humidity. They found that the vapor-induced phase separation gave the final fibers a porous structure, and these pores formed inside the fiber when a low volatility solvent (DMF) was used. Unlike in the above-mentioned studies, the pores in this case tended to develop on the fiber surfaces when a highly volatile solvent (THF) was used.

Water, as a nonsolvent, can also be directly added into the polymer solution to fabricate porous NFs. Yu et al. [145] prepared porous fibers by electrospinning a PAN/DMF/H_2O solution. Here, water acted as the nonsolvent to induce phase separation and to generate a porous structure. The specific surface area and the diameter of the porous fibers expanded with increases in water content and in polymer concentration.

Shen et al. [146] applied mineral oil as both the nonsolvent and the template to fabricate Sn nanoparticle-loaded PCNFs by electrospinning. When used as the anode material for an LIB, the Sn nanoparticle-loaded PCNFs exhibited a higher discharge capacity (774 mAh g^{-1} over 200 cycles, at a high current density of 0.8 A g^{-1}) than the Sn-CNF composite prepared without mineral oil.

The solvent-induced phase separation method for fabricating porous electrospun fibers is facile and cost-effective, because it does not require additive or post-treatment. By varying the composition of the solvent mixtures or importing nonsolvents, we can obtain porous NFs with different morphologies. But this method is less powerful in that the pores always form on the fiber surfaces due to the flash vaporization of the solvent.

Activation method based on electrospinning

The activation method is traditionally used for preparing porous carbon materials, and this approach involves either a physical or chemical activation method. After activation, the obtained electrospun carbon NFs present an abundance of micropores and a large specific surface area, which is favorable for transport of electrons and ions. Table 4 lists a series of activated electrospun PCNFs that have been applied in electrochemical energy storage devices.

Physical activation based on electrospinning

The physical activation method normally uses oxidizing gases such as steam [84, 105, 147–154], CO_2 [155–157] or air [158–160] to react with carbon. The disordered carbon is oxidation-etched to generate pores and develop microporous structures within the carbon materials. The activation efficiency of disordered carbon is relatively low, because it relies on the oxidation of carbon atoms to form a porous structure, and the temperature of carbonization and activation is very high (generally above 800 °C) [151, 153, 156–158].

Steam is often used to activate carbon NFs. Kim and Yang [147] used PAN as the carbon source and fabricated NFs by electrospinning in association with carbonization and activation by 30 vol% steam under a nitrogen flow. The as-obtained PCNFs, after being activated at 700 °C, provided a highest specific surface area of 1230 m^2 g^{-1}, and a maximum specific capacitance of 173 F g^{-1} when used as the electrode for an SC at low current density (10 mA g^{-1}). This result was mainly due to the high volume fraction of micropores. However, at the high current density of 1000 mA g^{-1}, the PCNFs activated at 800 °C exhibited a maximum specific capacitance of 120 F g^{-1}, because of the enhanced volume fraction of the mesopores. This outcome could be explained by the tendency of ions in the mesopores to respond faster at a higher current density than the ions in the micropores, which would lead to a higher specific capacitance.

In addition to the water in steam, the oxygen in air can serve as a simple activator. Li et al. [159] introduced air into the Ar flow during the carbonization process for preparing highly porous carbon NFs. The as-obtained porous carbon NFs were directly used as the anode material for an LIB, which delivered a reversible capacity of 1780 mAh g^{-1} after 40 cycles at 50 mA g^{-1}. When applied in LABs [157], the CO_2-actived carbon nanofibers (ACNF) network provided a novel pathway for O_2 across the cathode, and the mesopores introduced by activation acted as additional nucleation sites for Li_2O_2 formation, thereby

Table 4 A series of PCNFs obtained via activation

Purpose	Precursor	Activation	Specific surface area (m^2 g^{-1})	Electrochemical performance	References
EDLCs	PAN	H_2O	1230	173 F g^{-1} at 10 mA g^{-1}	[147]
EDLCs	PI	H_2O	1453	175 F g^{-1} at 1000 mA g^{-1}	[148]
EDLCs	PBI	H_2O	1220	202 F g^{-1} at 1 mA cm^{-2}	[149, 150]
EDLCs	PAN, PMMA	H_2O	1051.65	~120 F g^{-1} after 100 cycles at 20 mA cm^{-2}	[84]
EDLCs	PAN	H_2O	1255.6	58.02 F g^{-1} at 20 mA cm^{-2}	[151]
EDLCs	PAN	H_2O	1386.91	91.95 F g^{-1} at 1 mA cm^{-2}	[152]
LIBs	PAN	NH_3, H_2O	1198, 1056	1150 mAh g^{-1}, 513 mAh g^{-1} after 50 cycles at 50 mA g^{-1}	[153]
EDLCs	PAN–$Zn(Ac)_2$	H_2O	1404	178.2 F g^{-1} at 1 mA cm^{-2}	[154]
EDLCs	PAN, PMMA–$Ru(acac)_3$	H_2O	1552.2	180.2 F g^{-1} at 1 mA cm^{-2}	[105]
EDLCs	PAN	CO_2	705	175 F g^{-1} at 50 A g^{-1}	[155]
EDLCs	PAN	CO_2	712	228 F g^{-1} at 2 mV s^{-1}	[156]
LABs	PAN	CO_2	709	6099 mAh g^{-1} at 200 mA g^{-1}	[157]
EDLCs	PAN	Air	–	263.7 F g^{-1} at 100 mA g^{-1}	[158]
LIBs	PAN	Air	583	1550 mAh g^{-1} after 600 cycles at 500 mA g^{-1}	[159]
LIBs	PAN–$Fe(acac)_3$	Air	542.6	717.2 mAh g^{-1} after 100 cycles at 500 mA g^{-1}	[160]
LIBs	PAN, PMMA	KOH	1840	~1150 mAh g^{-1} after 70 cycles at 0.1 A g^{-1}	[125]
EDLCs	PF/PVA	KOH	1317	209 F g^{-1} at 20 A g^{-1}	[161]
EDLCs	PAN	$ZnCl_2$	550	140 F g^{-1} at 10 mV s^{-1}	[162]

leading to an increased discharge capacity (Fig. 8). After discharge, the ACNF cathode showed a layer-like morphology, and the nonactivated CNF showed a rugged surface. This outcome reflected the influence of numerous mesopores, which allowed Li_2O_2 to be homogeneously adsorbed onto the surface of the ACNF, while the CNF showed a relatively smooth surface that allowed easy migration of Li_2O_2 on the surface, thereby producing poorer cycling stability.

The oxidizing gases can react not only with carbon atoms, but they can also act as nitrogen sources to produce nitrogen-doped carbon materials. Nan et al. [153] prepared fiber networks by electrospinning a PAN/melamine solution. The electrospun fiber networks were carbonized in nitrogen and activated by ammonia to obtain a nitrogen-enriched porous carbon nanofibers (NPCNFs) networks with a specific surface area of 1198 m^2 g^{-1}, which was higher than that of steam-activated NPCNFs (1056 m^2 g^{-1}). When directly used as an LIB anode without a binder, the NPCNFs exhibited a reversible charge capacity of 1323 mAh g^{-1} in the first cycle and 1150 mAh g^{-1} in the 50th cycle (50 mA g^{-1}).

Chemical activation based on electrospinning

The chemical activation method generally uses chemicals such as KOH [125, 161] and $ZnCl_2$ [162] as the activators. These activators need to be removed by washing with acid or water. Ma et al. [161] fabricated phenolic-based activated carbon NFs paper by KOH activation. First, the as-spun phenolic fibers were immersed in KOH solutions of various concentrations for KOH coating. Then, carbon NFs paper was obtained by a one-step heat treatment. The treatment with KOH not only increased the porosity of the carbon NFs, but it also stimulated the surface oxygen functional groups to act as electrochemically active species. As a result, the as-obtained material, when used as the flexible electrode for an SC exhibited a high specific capacitance (362 F g^{-1}).

The chemical activator had a strong capability for etching the carbon precursor, and it could bring about uniform, abundant micropores, thereby leading to a high specific surface area and promoting the surface oxygen-containing functionality. As a result, the large specific surface area and the increased conductivity attributed to high graphitization effectively facilitated the electrochemical storage performance of the electrospun fibers [163].

Conclusions and challenges

The electrospinning technique is a low-cost and scalable method for producing 1D continuous NFs, and it can be adopted to fabricate 1D porous NFs for electrochemical energy storage devices. The as-fabricated porous NFs exhibit large specific surface

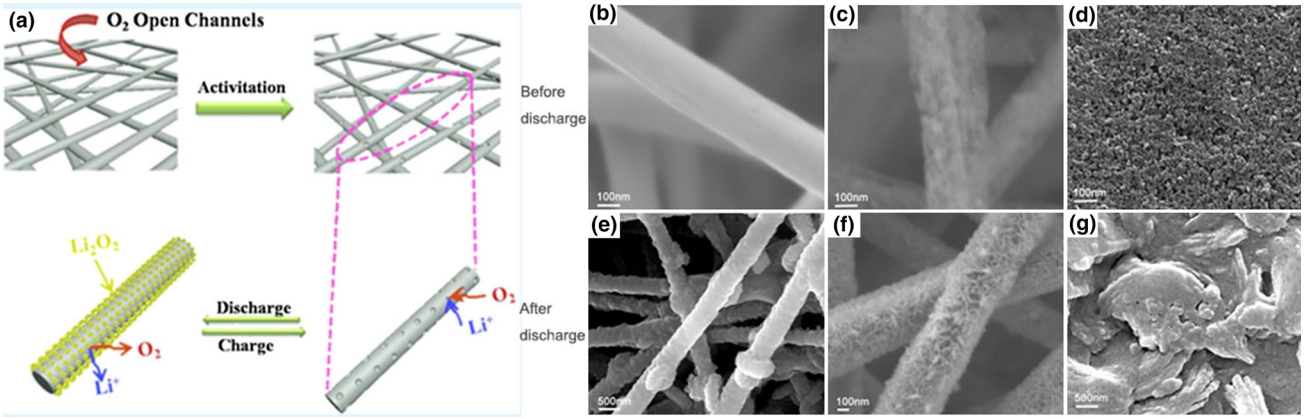

Figure 8 **a** Schematic illustration of a CO_2-activated carbon nanofibers network used in LABs. The SEM images are of CNF cathodes (**b**, **e**), ACNF cathodes (**c**, **f**) and BP 2000 composite cathodes (**d**, **g**) before and after discharge. Images reprinted with permission from Ref. [156]. Copyright 2016, American Chemical Society.

areas, and they allow rapid transport of electrons and ions. In addition, the void spaces in the porous NFs can effectively buffer the expansion of volume during the process of charging and discharging the electrode material. There are several methods for preparing 1D porous materials based on electrospinning, including the polymer template method, the hard (nanoparticles) template method, the solvent-induced and nonsolvent-induced methods, and the activation method. All of these methods can be applied to fabricate both PCNFs and composite NFs. The polymer template method, however, is only applicable for fabricating porous metal oxide NFs that are confined in 1D polymer fibers after removing the polymer template. By properly combining these methods with calcination and post-treatment, one can obtain highly porous NFs with high specific surface areas and unique porous structures. The as-obtained porous NFs, when used as the anode materials for LIBs, LABs, LSBs, NIBs or SCs, exhibit excellent electrochemical performance. However, some challenges still remain in developing 1D porous fibers and their composite structures:

1. It is important to develop PCNFs films with a naturally hierarchical porous structure, as this type of structure is needed to fabricate electrodes for energy storage devices without a binder. It is also important to broaden the range of porous PCNFs films prepared by electrospinning to oil–water separation, catalysis and tissue engineering.
2. It is imperative to further explore the potential for combining electrospinning techniques with other methods such as calcining or activation, as a means to acquire novel 1D porous fibers and their composite structures with significantly improved electrochemical performances.
3. More in-depth researches are necessary to realize better control in the preparation of porous NFs, thereby promoting the greater application of electrospun porous NFs in engineering.

Acknowledgements

The authors appreciate the financial support from the National Natural Science Foundation of China (Grant No. 20971037). The Key Project of He'nan Educational Committee (14A150005), the Program for Innovative Research Team from the University of Henan Province (16IRTSTHN015) and the Henan Key Scientific and Technological Project (152102210056).

Compliance with ethical standards

Conflict of interest The authors declare that they have no conflict of interest.

References

[1] Bruce PG, Freunberger SA, Hardwick LJ, Tarascon JM (2012) Li–O_2 and Li–S batteries with high energy storage. Nat Mater 11(1):19–29. doi:10.1038/nmat3191

[2] Zhang BA, Kang FY, Tarascon JM, Kim JK (2016) Recent advances in electrospun carbon nanofibers and their application in electrochemical energy storage. Prog Mater Sci 76:319–380. doi:10.1016/j.pmatsci.2015.08.002

[3] Goodenough JB (2014) Electrochemical energy storage in a sustainable modern society. Energy Environ Sci 7(1):14–18. doi:10.1039/C3EE42613K

[4] Arico AS, Bruce P, Scrosati B, Tarascon JM, van Schalkwijk W (2005) Nanostructured materials for advanced energy conversion and storage devices. Nat Mater 4(5):366–377. doi:10.1038/nmat1368

[5] Hochbaum AI, Chen R, Delgado RD, Liang W, Garnett EC, Najarian M, Majumdar A, Yang P (2008) Enhanced thermoelectric performance of rough silicon nanowires. Nature 451(7175):163–167. doi:10.1038/nature06381

[6] Mai L, Tian X, Xu X, Chang L, Xu L (2014) Nanowire electrodes for electrochemical energy storage devices. Chem Rev 114(23):11828–11862. doi:10.1021/cr500177a

[7] Palmer LC, Stupp SI (2008) Molecular self-assembly into one-dimensional nanostructures. Acc Chem Res 41(12):1674–1684. doi:10.1021/ar8000926

[8] Xia YN, Yang PD, Sun YG, Wu YY, Mayers B, Gates B, Yin YD, Kim F, Yan YQ (2003) One-dimensional nanostructures: synthesis, characterization, and applications. Adv Mater 15(5):353–389. doi:10.1002/adma.200390087

[9] Zheng Z, Cheng Y, Yan X, Wang R, Zhang P (2014) Enhanced electrochemical properties of graphene-wrapped $ZnMn_2O_4$ nanorods for lithium-ion batteries. J Mater Chem A 2(1):149–154. doi:10.1039/C3TA13511J

[10] Aravindan V, Sundaramurthy J, Suresh Kumar P, Lee Y-S, Ramakrishna S, Madhavi S (2015) Electrospun nanofibers: a prospective electro-active material for constructing high performance Li-ion batteries. Chem Commun 51(12):2225–2234. doi:10.1039/C4CC07824A

[11] Zhang JH, Zhao YR, Han SY, Chen CX, Xu H (2014) Self-assembly of surfactant-like peptides and their applications. Sci China Chem 57(12):1634–1645. doi:10.1007/s11426-014-5234-4

[12] Ryu J, Kim S-W, Kang K, Park CB (2010) Mineralization of self-assembled peptide nanofibers for rechargeable lithium ion batteries. Adv Mater 22(48):5537–5541. doi:10.1002/adma.201000669

[13] Supothina S, Rattanakam R, Tawkaew S (2012) Hydrothermal synthesis and photocatalytic activity of anatase TiO_2 nanofiber. J Nanosci Nanotechnol 12(6):4998–5003. doi:10.1166/jnn.2012.4939

[14] Li J, Zhou Z, Zhu L, Xu K, Tang H (2007) Salt effects on crystallization of titanate and the tailoring of its nanostructures. J Phys Chem C 111(45):16768–16773. doi:10.1021/jp0755239

[15] Ma H, Zhang S, Ji W, Tao Z, Chen J (2008) Alpha-CuV_2O_6 nanowires: hydrothermal synthesis and primary lithium battery application. J Am Chem Soc 130(15):5361–5367. doi:10.1021/ja800109u

[16] Wu CG, Bein T (1994) Conducting polyaniline filaments in a mesoporous channel host. Science 264(5166):1757–1759. doi:10.1126/science.264.5166.1757

[17] Li NC, Martin CR (2001) A high-rate, high-capacity, nanostructured Sn-based anode prepared using sol-gel template synthesis. J Electrochem Soc 148(2):A164–A170. doi:10.1149/1.1342167

[18] Fan ZJ, Yan J, Wei T, Ning GQ, Zhi LJ, Liu JC, Cao DX, Wang GL, Wei F (2011) Nanographene-constructed carbon nanofibers grown on graphene sheets by chemical vapor deposition: high-performance anode materials for lithium ion batteries. ACS Nano 5(4):2787–2794. doi:10.1021/nn200195k

[19] Meier C, Welland ME (2011) Wet-spinning of amyloid protein nanofibers into multifunctional high-performance biofibers. Biomacromolecules 12(10):3453–3459. doi:10.1021/bm2005752

[20] Zhang XW, Lu Y (2014) Centrifugal spinning: an alternative approach to fabricate nanofibers at high speed and low cost. Polym Rev 54(4):677–701. doi:10.1080/15583724.2014.935858

[21] Weng BC, Xu FH, Alcoutlabi M, Mao YB, Lozano K (2015) Fibrous cellulose membrane mass produced via forcespinning for lithium-ion battery separators. Cellulose 22(2):1311–1320. doi:10.1007/s10570-015-0564-8

[22] Agubra VA, Zuniga L, De la Garza D, Gallegos L, Pokhrel M, Alcoutlabi M (2016) Forcespinning: a new method for the mass production of Sn/C composite nanofiber anodes for lithium ion batteries. Solid State Ionics 286:72–82. doi:10.1016/jssi.2015.12.020

[23] Zander NE (2015) Formation of melt and solution spun polycaprolactone fibers by centrifugal spinning. J Appl Polym Sci 132(2):41269. doi:10.1002/App.41269

[24] O'Haire T, Russell SJ, Carr CM (2016) Centrifugal melt spinning of polyvinylpyrrolidone (PVP)/triacontene copolymer fibres. J Mater Sci 51(16):7512–7522. doi:10.1007/s10853-016-0030-5

[25] Inagaki M, Yang Y, Kang F (2012) Carbon nanofibers prepared via electrospinning. Adv Mater 24(19):2547–2566. doi:10.1002/adma.201104940

[26] Kalluri S, Seng KH, Guo ZP, Liu HK, Dou SX (2013) Electrospun lithium metal oxide cathode materials for lithium-ion batteries. RSC Adv 3(48):25576–25601. doi:10.1039/c3ra45414b

[27] Li D, Xia Y (2004) Electrospinning of nanofibers: reinventing the wheel? Adv Mater 16(14):1151–1170. doi:10.1002/adma.200400719

[28] Formhals A, Formhals A (1934) Process and apparatus for preparing artificial threads. U S Patent
[29] Taylor G (1969) Electrically driven jets. Proc R Soc A 313(1515):453–475. doi:10.1098/rspa.1969.0205
[30] Kong CS, Lee TH, Lee SH, Kim HS (2007) Nano-web formation by the electrospinning at various electric fields. J Mater Sci 42(19):8106–8112. doi:10.1007/s10853-007-1734-3
[31] Shawon J, Sung C (2004) Electrospinning of polycarbonate nanofibers with solvent mixtures THF and DMF. J Mater Sci 39(14):4605–4613. doi:10.1023/B:JMSC.0000034155.93428.ea
[32] Li D, Wang J, Dong X, Yu W, Liu G (2013) Fabrication and luminescence properties of YF_3:Eu^{3+} hollow nanofibers via coaxial electrospinning combined with fluorination technique. J Mater Sci 48(17):5930–5937. doi:10.1007/s10853-013-7388-4
[33] De Vrieze S, Van Camp T, Nelvig A, Hagström B, Westbroek P, De Clerck K (2008) The effect of temperature and humidity on electrospinning. J Mater Sci 44(5):1357–1362. doi:10.1007/s10853-008-3010-6
[34] De Schoenmaker B, Van der Schueren L, Zugle R, Goethals A, Westbroek P, Kiekens P, Nyokong T, De Clerck K (2012) Effect of the relative humidity on the fibre morphology of polyamide 4.6 and polyamide 6.9 nanofibres. J Mater Sci 48(4):1746–1754. doi:10.1007/s10853-012-6934-9
[35] De Schoenmaker B, Goethals A, Van der Schueren L, Rahier H, De Clerck K (2012) Polyamide 6.9 nanofibres electrospun under steady state conditions from a solvent/non-solvent solution. J Mater Sci 47(9):4118–4126. doi:10.1007/s10853-012-6266-9
[36] Matabola KP, Moutloali RM (2013) The influence of electrospinning parameters on the morphology and diameter of poly(vinyledene fluoride) nanofibers—effect of sodium chloride. J Mater Sci 48(16):5475–5482. doi:10.1007/s10853-013-7341-6
[37] Jung JW, Lee CL, Yu S, Kim ID (2016) Electrospun nanofibers as a platform for advanced secondary batteries: a comprehensive review. J Mater Chem A 4(3):703–750. doi:10.1039/c5ta06844d
[38] Jalvandi J, White M, Truong YB, Gao Y, Padhye R, Kyratzis IL (2015) Release and antimicrobial activity of levofloxacin from composite mats of poly(ε-caprolactone) and mesoporous silica nanoparticles fabricated by core–shell electrospinning. J Mater Sci 50(24):7967–7974. doi:10.1007/s10853-015-9361-x
[39] Pampal ES, Stojanovska E, Simon B, Kilic A (2015) A review of nanofibrous structures in lithium ion batteries. J Power Sources 300:199–215. doi:10.1016/j.jpowsour.2015.09.059
[40] Khalil A, Lalia BS, Hashaikeh R (2016) Nickel oxide nanocrystals as a lithium-ion battery anode: structure-performance relationship. J Mater Sci 51(14):6624–6638. doi:10.1007/s10853-016-9946-z
[41] Qiu Y, Geng Y, Yu J, Zuo X (2013) High-capacity cathode for lithium-ion battery from $LiFePO_4$/(C + Fe_2P) composite nanofibers by electrospinning. J Mater Sci 49(2):504–509. doi:10.1007/s10853-013-7727-5
[42] Sandhya CP, John B, Gouri C (2013) Synthesis and electrochemical characterisation of electrospun lithium titanate ultrafine fibres. J Mater Sci 48(17):5827–5832. doi:10.1007/s10853-013-7375-9
[43] Gao C, Li X, Lu B, Chen L, Wang Y, Teng F, Wang J, Zhang Z, Pan X, Xie E (2012) A facile method to prepare SnO_2 nanotubes for use in efficient SnO_2–TiO_2 core–shell dye-sensitized solar cells. Nanoscale 4(11):3475–3481. doi:10.1039/c2nr30349c
[44] Yang T, Lu B (2014) Highly porous structure strategy to improve the SnO_2 electrode performance for lithium-ion batteries. Phys Chem Chem Phys 16(9):4115–4121. doi:10.1039/c3cp54144d
[45] Kundu M, Liu LF (2015) Binder-free electrodes consisting of porous NiO nanofibers directly electrospun on nickel foam for high-rate supercapacitors. Mater Lett 144:114–118. doi:10.1016/j.matlet.2015.01.032
[46] Wang B, Cheng JL, Wu YP, Wang D, He DN (2012) Porous NiO fibers prepared by electrospinning as high performance anode materials for lithium ion batteries. Electrochem Commun 23:5–8. doi:10.1016/j.elecom.2012.07.003
[47] Aravindan V, Kumar PS, Sundaramurthy J, Ling WC, Ramakrishna S, Madhavi S (2013) Electrospun NiO nanofibers as high performance anode material for Li-ion batteries. J Power Sources 227:284–290. doi:10.1016/j.jpowsour.2012.11.050
[48] Qiao L, Wang X, Qiao L, Sun X, Li X, Zheng Y, He D (2013) Single electrospun porous NiO–ZnO hybrid nanofibers as anode materials for advanced lithium-ion batteries. Nanoscale 5(7):3037–3042. doi:10.1039/c3nr34103h
[49] Wang HG, Zhou YQ, Shen Y, Li YH, Zuo QH, Duan Q (2015) Fabrication, formation mechanism and the application in lithium-ion battery of porous Fe_2O_3 nanotubes via single-spinneret electrospinning. Electrochim Acta 158:105–112. doi:10.1016/j.electacta.2015.01.149
[50] Cui ZT, Wang SG, Zhang YH, Cao MH (2015) High-performance lithium storage of Co_3O_4 achieved by constructing porous nanotube structure. Electrochim Acta 182:507–515. doi:10.1016/j.electacta.2015.09.120
[51] Wang Y, Takahashi K, Lee K, Cao GZ (2006) Nanostructured vanadium oxide electrodes for enhanced lithium-ion

intercalation. Adv Funct Mater 16(9):1133–1144. doi:10.1002/adfm.200500662

[52] Zhai T, Liu H, Li H, Fang X, Liao M, Li L, Zhou H, Koide Y, Bando Y, Golberg D (2010) Centimeter-long V_2O_5 nanowires: from synthesis to field-emission, electrochemical, electrical transport, and photoconductive properties. Adv Mater 22(23):2547–2552. doi:10.1002/adma.200903586

[53] Cheah YL, Gupta N, Pramana SS, Aravindan V, Wee G, Srinivasan M (2011) Morphology, structure and electrochemical properties of single phase electrospun vanadium pentoxide nanofibers for lithium ion batteries. J Power Sources 196(15):6465–6472. doi:10.1016/j.jpowsour.2011.03.039

[54] Wang HG, Ma DL, Huang Y, Zhang XB (2012) Electrospun V_2O_5 nanostructures with controllable morphology as high-performance cathode materials for lithium-ion batteries. Chem Eur J 18(29):8987–8993. doi:10.1002/chem.201200434

[55] Yu DM, Chen CG, Xie SH, Liu YY, Park K, Zhou XY, Zhang QF, Li JY, Cao GZ (2011) Mesoporous vanadium pentoxide nanofibers with significantly enhanced Li-ion storage properties by electrospinning. Energy Environ Sci 4(3):858–861. doi:10.1039/c0ee00313a

[56] Lee DJ, Lee H, Ryou MH, Han GB, Lee JN, Song J, Choi J, Cho KY, Lee YM, Park JK (2013) Electrospun three-dimensional mesoporous silicon nanofibers as an anode material for high-performance lithium secondary batteries. ACS Appl Mater Interfaces 5(22):12005–12010. doi:10.1021/am403798a

[57] Yoo JK, Kim J, Lee H, Choi J, Choi MJ, Sim DM, Jung YS, Kang K (2013) Porous silicon nanowires for lithium rechargeable batteries. Nanotechnology 24(42):424008. doi:10.1088/0957-4484/24/42/424008

[58] Teh PF, Sharma Y, Pramana SS, Srinivasan M (2011) Nanoweb anodes composed of one-dimensional, high aspect ratio, size tunable electrospun $ZnFe_2O_4$ nanofibers for lithium ion batteries. J Mater Chem 21(38):14999–15008. doi:10.1039/c1jm12088c

[59] Luo W, Hu XL, Sun YM, Huang YH (2012) Electrospun porous $ZnCo_2O_4$ nanotubes as a high-performance anode material for lithium-ion batteries. J Mater Chem 22(18):8916–8921. doi:10.1039/c2jm00094f

[60] Yang GR, Xu X, Yan W, Yang HH, Ding SJ (2014) Facile synthesis of interwoven $ZnMn_2O_4$ nanofibers by electrospinning and their performance in Li-ion batteries. Mater Lett 128:336–339. doi:10.1016/j.matlet.2014.04.157

[61] Cherian CT, Sundaramurthy J, Reddy MV, Suresh Kumar P, Mani K, Pliszka D, Sow CH, Ramakrishna S, Chowdari BV (2013) Morphologically robust $NiFe_2O_4$ nanofibers as high capacity Li-ion battery anode material. ACS Appl Mater Interfaces 5(20):9957–9963. doi:10.1021/am401779p

[62] Wang L, Xiao QZ, Li ZH, Lei GT, Zhang P, Wu LJ (2012) Synthesis of $Li_4Ti_5O_{12}$ fibers as a high-rate electrode material for lithium-ion batteries. J Solid State Electrochem 16(10):3307–3313. doi:10.1007/s10008-012-1776-6

[63] Xu HH, Shu J, Hu XL, Sun YM, Luo W, Huang YH (2013) Electrospun porous $LiNb_3O_8$ nanofibers with enhanced lithium-storage properties. J Mater Chem A 1(47):15053–15059. doi:10.1039/c3ta13386a

[64] Li L, Peng S, Wang J, Cheah YL, Teh P, Ko Y, Wong C, Srinivasan M (2012) Facile approach to prepare porous $CaSnO_3$ nanotubes via a single spinneret electrospinning technique as anodes for lithium ion batteries. ACS Appl Mater Interfaces 4(11):6005–6012. doi:10.1021/am301664e

[65] Niu C, Meng J, Wang X, Han C, Yan M, Zhao K, Xu X, Ren W, Zhao Y, Xu L, Zhang Q, Zhao D, Mai L (2015) General synthesis of complex nanotubes by gradient electrospinning and controlled pyrolysis. Nat Commun 6:7402. doi:10.1038/ncomms8402

[66] Wang Q, Chen D, Zhang D (2015) Electrospun porous $CuCo_2O_4$ nanowire network electrode for asymmetric supercapacitors. RSC Adv 5(117):96448–96454. doi:10.1039/c5ra21170k

[67] Zhou G, Zhu J, Chen YJ, Mei L, Duan XC, Zhang GH, Chen LB, Wang TH, Lu BA (2014) Simple method for the preparation of highly porous $ZnCo_2O_4$ nanotubes with enhanced electrochemical property for supercapacitor. Electrochim Acta 123:450–455. doi:10.1016/j.electacta.2014.01.018

[68] Zhu JD, Lu Y, Chen C, Ge YQ, Jasper S, Leary JD, Li DW, Jiang MJ, Zhang XW (2016) Porous one-dimensional carbon/iron oxide composite for rechargeable lithium-ion batteries with high and stable capacity. J Alloys Compd 672:79–85. doi:10.1016/j.jallcom.2016.02.160

[69] Xu HH, Hu XL, Sun YM, Luo W, Chen CJ, Liu Y, Huang YH (2014) Highly porous $Li_4Ti_5O_{12}$/C nanofibers for ultrafast electrochemical energy storage. Nano Energy 10:163–171. doi:10.1016/j.nanoen.2014.09.003

[70] Hwang SM, Lim YG, Kim JG, Heo YU, Lim JH, Yamauchi Y, Park MS, Kim YJ, Dou SX, Kim JH (2014) A case study on fibrous porous SnO_2 anode for robust, high-capacity lithium-ion batteries. Nano Energy 10:53–62. doi:10.1016/j.nanoen.2014.08.020

[71] Li LM, Yin XM, Liu SA, Wang YG, Chen LB, Wang TH (2010) Electrospun porous SnO_2 nanotubes as high capacity anode materials for lithium ion batteries. Electrochem Commun 12(10):1383–1386. doi:10.1016/j.elecom.2010.07.026

[72] Huang HM, Zhang SQ, Wang W, Wang C, Jie YU (2012) Fabrication of electrospun porous SnO_2 nanofibers as anodes materials for lithium-ion batteries. Chem J Chin Univ 33(7):1619–1623. doi:10.3969/j.issn.0251-0790.2012.07.045

[73] Lei DN, Qu BH, Lin HT, Wang TH (2015) Facile approach to prepare porous GeO_2/SnO_2 nanofibers via a single spinneret electrospinning technique as anodes for lithium-ion batteries. Ceram Int 41(8):10308–10313. doi:10.1016/j.ceramint.2015.04.085

[74] Sun X, Huang Y, Zong M, Wu H, Ding X (2015) Preparation of porous SnO_2/ZnO nanotubes via a single spinneret electrospinning technique as anodes for lithium ion batteries. J Mater Sci: Mater Electron 27(3):2682–2686. doi:10.1007/s10854-015-4077-x

[75] Jayaraman S, Aravindan V, Suresh Kumar P, Ling WC, Ramakrishna S, Madhavi S (2013) Synthesis of porous $LiMn_2O_4$ hollow nanofibers by electrospinning with extraordinary lithium storage properties. Chem Commun 49(59):6677–6679. doi:10.1039/c3cc43874k

[76] Zhou H, Ding X, Liu G, Gao Z, Xu G, Wang X (2015) Characterization of cathode from $LiNi_XMn_{2-X}O_4$ nanofibers by electrospinning for Li-ion batteries. RSC Adv 5(130):108007–108014. doi:10.1039/C5RA21884E

[77] Li PF, Zhang JK, Yu QL, Qiao JS, Wang ZH, Rooney D, Sun W, Sun KN (2015) One-dimensional porous $La_{0.5}Sr_{0.5}CoO_{2.91}$ nanotubes as a highly efficient electrocatalyst for rechargeable lithium-oxygen batteries. Electrochim Acta 165:78–84. doi:10.1016/j.electacta.2015.03.005

[78] Li L, Shen L, Nie P, Pang G, Wang J, Li H, Dong S, Zhang X (2015) Porous $NiCo_2O_4$ nanotubes as noble metal-free effective bifunctional catalysts for rechargeable Li–O_2 batteries. J Mater Chem A 3(48):24309–24314. doi:10.1039/C5TA07856C

[79] Jo E, Yeo JG, Kim DK, Oh JS, Hong CK (2014) Preparation of well-controlled porous carbon nanofiber materials by varying the compatibility of polymer blends. Polym Int 63(8):1471–1477. doi:10.1002/pi.4645

[80] Jing LI, Qiao H, Wei QF (2011) Porous carbon nanofibers prepared by electrospinning technique. Battery Bimonthly 41(3):132–134

[81] Wei K, Kim KO, Song KH, Kang CY, Lee JS, Gopiraman M, Kim IS (2016) Nitrogen- and oxygen-containing porous ultrafine carbon nanofiber: a highly flexible electrode material for supercapacitor. J Mater Sci Technol. doi:10.1016/j.jmst.2016.03.014

[82] Peng YT, Lo CT (2015) Electrospun porous carbon nanofibers as lithium ion battery anodes. J Solid State Electrochem 19(11):3401–3410. doi:10.1007/s10008-015-2976-7

[83] Kim C, Jeong YI, Ngoc BT, Yang KS, Kojima M, Kim YA, Endo M, Lee JW (2007) Synthesis and characterization of porous carbon nanofibers with hollow cores through the thermal treatment of electrospun copolymeric nanofiber webs. Small 3(1):91–95. doi:10.1002/smll.200600243

[84] Kim BH, Yang KS, Ferraris JP (2012) Highly conductive, mesoporous carbon nanofiber web as electrode material for high-performance supercapacitors. Electrochim Acta 75:325–331. doi:10.1016/j.electacta.2012.05.004

[85] Lai CC, Lo CT (2015) Preparation of nanostructural carbon nanofibers and their electrochemical performance for supercapacitors. Electrochim Acta 183:85–93. doi:10.1016/j.electacta.2015.02.143

[86] Wang Q, Cao Q, Wang XY, Jing B, Kuang H, Zhou L (2013) Dual template method to prepare hierarchical porous carbon nanofibers for high-power supercapacitors. J Solid State Electrochem 17(10):2731–2739. doi:10.1007/s10008-013-2166-4

[87] Park GS, Lee JS, Kim ST, Park S, Cho J (2013) Porous nitrogen doped carbon fiber with churros morphology derived from electrospun bicomponent polymer as highly efficient electrocatalyst for Zn–air batteries. J Power Sources 243:267–273. doi:10.1016/j.jpowsour.2013.06.025

[88] Qin XY, Zhang HR, Wu JX, Chu XD, He YB, Han CP, Miao C, Wang SA, Li BH, Kang FY (2015) Fe_3O_4 nanoparticles encapsulated in electrospun porous carbon fibers with a compact shell as high-performance anode for lithium ion batteries. Carbon 87:347–356. doi:10.1016/j.carbon.2015.02.044

[89] Zeng Y, Li X, Jiang S, He S, Fang H, Hou H (2015) Free-standing mesoporous electrospun carbon nanofiber webs without activation and their electrochemical performance. Mater Lett 161:587–590. doi:10.1016/j.matlet.2015.08.154

[90] Zhang LJ, Han LL, Liu S, Zhang C, Liu SX (2015) High-performance supercapacitors based on electrospun multi-channel carbon nanofibers. RSC Adv 5(130):107313–107317. doi:10.1039/c5ra23338k

[91] Ji L, Zhang X (2009) Fabrication of porous carbon nanofibers and their application as anode materials for rechargeable lithium-ion batteries. Nanotechnology 20(15):155705. doi:10.1088/0957-4484/20/15/155705

[92] Yang Y, Centrone A, Chen L, Simeon F, Hatton TA, Rutledge GC (2011) Highly porous electrospun polyvinylidene fluoride (PVDF)-based carbon fiber. Carbon 49(11):3395–3403. doi:10.1016/j.carbon.2011.04.015

[93] Tran C, Kalra V (2013) Fabrication of porous carbon nanofibers with adjustable pore sizes as electrodes for supercapacitors. J Power Sources 235:289–296. doi:10.1016/j.jpowsour.2013.01.080

[94] Li W, Zeng L, Yang Z, Gu L, Wang J, Liu X, Cheng J, Yu Y (2014) Free-standing and binder-free sodium-ion electrodes with ultralong cycle life and high rate performance based on porous carbon nanofibers. Nanoscale 6(2):693–698. doi:10.1039/c3nr05022j

[95] Huang K, Yao Y, Yang X, Chen Z, Li M (2016) Fabrication of flexible hierarchical porous nitrogen-doped carbon nanofiber films for application in binder-free supercapacitors. Mater Chem Phys 169:1–5. doi:10.1016/j.matchemphys.2015.11.024

[96] Kim BH, Yang KS, Woo HG (2012) Physical and electrochemical studies of polyphenylsilane-derived porous carbon nanofibers produced via electrospinning. Electrochim Acta 59:202–206. doi:10.1016/j.electacta.2011.10.057

[97] Kim BH, Yang KS, Woo HG, Oshida K (2011) Supercapacitor performance of porous carbon nanofiber composites prepared by electrospinning polymethylhydrosiloxane (PMHS)/polyacrylonitrile (PAN) blend solutions. Synth Met 161(13–14):1211–1216. doi:10.1016/j.synthmet.2011.04.005

[98] Zhang ZY, Li XH, Wang CH, Fu SW, Liu YC, Shao CL (2009) Polyacrylonitrile and carbon nanofibers with controllable nanoporous structures by electrospinning. Macromol Mater Eng 294(10):673–678. doi:10.1002/mame.200900076

[99] Lee BS, Son SB, Park KM, Lee G, Oh KH, Lee SH, Yu WR (2012) Effect of pores in hollow carbon nanofibers on their negative electrode properties for a lithium rechargeable battery. ACS Appl Mater Interfaces 4(12):6702–6710. doi:10.1021/am301873d

[100] Tang X, Wei YH, Zhang HN, Yan FL, Zhuo M, Chen CM, Xiao PY, Liang JJ, Zhang M (2015) The positive influence of graphene on the mechanical and electrochemical properties of Sn_XSb-graphene-carbon porous mats as binder-free electrodes for Li^+ storage. Electrochim Acta 186:223–230. doi:10.1016/j.electacta.2015.10.170

[101] Chen C, Fu K, Lu Y, Zhu J, Xue L, Hu Y, Zhang X (2015) Use of a tin antimony alloy-filled porous carbon nanofiber composite as an anode in sodium-ion batteries. RSC Adv 5(39):30793–30800. doi:10.1039/C5RA01729G

[102] Li X, Chen Y, Zhou L, Mai Y-W, Huang H (2014) Exceptional electrochemical performance of porous TiO_2-carbon nanofibers for lithium ion battery anodes. J Mater Chem A 2(11):3875–3880. doi:10.1039/c3ta14646d

[103] Yang XJ, Teng DH, Liu BX, Yu YH, Yang XP (2011) Nanosized anatase titanium dioxide loaded porous carbon nanofiber webs as anode materials for lithium-ion batteries. Electrochem Commun 13(10):1098–1101. doi:10.1016/j.elecom.2011.07.007

[104] Yang KS, Kim CH, Kim BH (2015) Preparation and electrochemical properties of RuO_2-containing activated carbon nanofiber composites with hollow cores. Electrochim Acta 174:290–296. doi:10.1016/j.electacta.2015.05.176

[105] Yang KS, Kim BH (2015) Highly conductive, porous RuO_2/activated carbon nanofiber composites containing graphene for electrochemical capacitor electrodes. Electrochim Acta 186:337–344. doi:10.1016/j.electacta.2015.11.003

[106] Wu JX, Qin XY, Miao C, He YB, Liang GM, Zhou D, Liu M, Han CP, Li BH, Kang FY (2016) A honeycomb-cobweb inspired hierarchical core–shell structure design for electrospun silicon/carbon fibers as lithium-ion battery anodes. Carbon 98:582–591. doi:10.1016/j.carbon.2015.11.048

[107] Li XJ, Lei GT, Li ZH, Zhang Y, Xiao QZ (2014) Carbon-encapsulated Si nanoparticle composite nanofibers with porous structure as lithium-ion battery anodes. Solid State Ionics 261:111–116. doi:10.1016/j.ssi.2014.04.016

[108] Li WH, Yang ZZ, Jiang Y, Yu ZR, Gu L, Yu Y (2014) Crystalline red phosphorus incorporated with porous carbon nanofibers as flexible electrode for high performance lithium-ion batteries. Carbon 78:455–462. doi:10.1016/j.carbon.2014.07.026

[109] Yu Y, Gu L, Zhu CB, van Aken PA, Maier J (2009) Tin nanoparticles encapsulated in porous multichannel carbon microtubes: preparation by single-nozzle electrospinning and application as anode material for high-performance li-based batteries. J Am Chem Soc 131(44):15984–15985. doi:10.1021/ja906261c

[110] Meschini I, Nobili F, Mancini M, Marassi R, Tossici R, Savoini A, Focarete ML, Croce F (2013) High-performance Sn@carbon nanocomposite anode for lithium batteries. J Power Sources 226:241–248. doi:10.1016/j.jpowsour.2012.11.004

[111] Ji LW, Zhang XW (2010) Evaluation of Si/carbon composite nanofiber-based insertion anodes for new-generation rechargeable lithium-ion batteries. Energy Environ Sci 3(1):124–129. doi:10.1039/b912188a

[112] Ji LW, Zhang XW (2009) Fabrication of porous carbon/Si composite nanofibers as high-capacity battery electrodes. Electrochem Commun 11(6):1146–1149. doi:10.1016/j.elecom.2009.03.042

[113] Wang MS, Song WL, Wang J, Fan LZ (2015) Highly uniform silicon nanoparticle/porous carbon nanofiber hybrids towards free-standing high-performance anodes for lithium-ion batteries. Carbon 82:337–345. doi:10.1016/j.carbon.2014.10.078

[114] Dong Y, Lin HM, Zhou D, Niu H, Jin QM, Qu FY (2015) Synthesis of mesoporous graphitic carbon fibers with high

performance for supercapacitor. Electrochim Acta 159:116–123. doi:10.1016/j.electacta.2015.01.152

[115] Ji LW, Lin Z, Medford AJ, Zhang XW (2009) Porous carbon nanofibers from electrospun polyacrylonitrile/SiO_2 composites as an energy storage material. Carbon 47(14):3346–3354. doi:10.1016/j.carbon.2009.08.002

[116] Nan D, Wang JG, Huang ZH, Wang L, Shen WC, Kang FY (2013) Highly porous carbon nanofibers from electrospun polyimide/SiO_2 hybrids as an improved anode for lithium-ion batteries. Electrochem Commun 34:52–55. doi:10.1016/j.elecom.2013.05.010

[117] Teng MM, Qiao JL, Li FT, Bera PK (2012) Electrospun mesoporous carbon nanofibers produced from phenolic resin and their use in the adsorption of large dye molecules. Carbon 50(8):2877–2886. doi:10.1016/j.carbon.2012.02.056

[118] An GH, Ahn HJ (2013) Activated porous carbon nanofibers using Sn segregation for high-performance electrochemical capacitors. Carbon 65:87–96. doi:10.1016/j.carbon.2013.08.002

[119] Liu ZY, Fu DY, Liu FF, Han GY, Liu CX, Chang YZ, Xiao YM, Li MY, Li SD (2014) Mesoporous carbon nanofibers with large cage-like pores activated by tin dioxide and their use in supercapacitor and catalyst support. Carbon 70:295–307. doi:10.1016/j.carbon.2014.01.011

[120] Cheng L, He JJ, Jin Y, Chen HY, Chen MH (2015) Single-walled carbon nanotube embedded porous carbon nanofiber with enhanced electrochemical capacitive performance. Mater Lett 144:123–126. doi:10.1016/j.matlet.2015.01.020

[121] Zhang XB, Chen MH, Zhang XG, Li QW (2010) Preparation of porous carbon nanofibers by electrospinning and their electrochemical capacitive behavior. Acta Phys Chim Sin 26(12):3169–3174. doi:10.3866/Pku.Whxb20101203

[122] Ji LW, Zhang XW (2009) Generation of activated carbon nanofibers from electrospun polyacrylonitrile-zinc chloride composites for use as anodes in lithium-ion batteries. Electrochem Commun 11(3):684–687. doi:10.1016/j.elecom.2009.01.018

[123] Zhang B, Xu ZL, He YB, Abouali S, Garakani MA, Heidari EK, Kang FY, Kim JK (2014) Exceptional rate performance of functionalized carbon nanofiber anodes containing nanopores created by (Fe) sacrificial catalyst. Nano Energy 4:88–96. doi:10.1016/j.nanoen.2013.12.011

[124] Chen YM, Lu ZG, Zhou LM, Mai YW, Huang HT (2012) Triple-coaxial electrospun amorphous carbon nanotubes with hollow graphitic carbon nanospheres for high- performance Li ion batteries. Energy Environ Sci 5(7):7898–7902. doi:10.1039/c2ee22085g

[125] Chen Y, Li X, Park K, Song J, Hong J, Zhou L, Mai YW, Huang H, Goodenough JB (2013) Hollow carbon-nanotube/carbon-nanofiber hybrid anodes for Li-ion batteries. J Am Chem Soc 135(44):16280–16283. doi:10.1021/ja408421n

[126] Nagamine S, Matsumoto T, Hikima Y, Ohshima M (2016) Fabrication of porous carbon nanofibers by phosphate-assisted carbonization of electrospun poly(vinyl alcohol) nanofibers. Mater Res Bull 79:8–13. doi:10.1016/j.materresbull.2016.01.009

[127] Zhang LJ, Jiang YZ, Wang LW, Zhang C, Liu SX (2016) Hierarchical porous carbon nanofibers as binder-free electrode for high-performance supercapacitor. Electrochim Acta 196:189–196. doi:10.1016/j.electacta.2016.02.050

[128] Karthikeyan KK, Biji P (2016) A novel biphasic approach for direct fabrication of highly porous, flexible conducting carbon nanofiber mats from polyacrylonitrile (PAN)/$NaHCO_3$ nanocomposite. Microporous Mesoporous Mater 224:372–383. doi:10.1016/j.micromeso.2015.12.055

[129] Liang QH, Ye L, Xu Q, Huang ZH, Kang FY, Yang QH (2015) Graphitic carbon nitride nanosheet-assisted preparation of N-enriched mesoporous carbon nanofibers with improved capacitive performance. Carbon 94:342–348. doi:10.1016/j.carbon.2015.07.001

[130] Zhou X, Wan LJ, Guo YG (2013) Electrospun silicon nanoparticle/porous carbon hybrid nanofibers for lithium-ion batteries. Small 9(16):2684–2688. doi:10.1002/smll.201202071

[131] Wang H, Lu X, Li L, Li B, Cao D, Wu Q, Li Z, Yang G, Guo B, Niu C (2016) Synthesis of SnO_2 versus Sn crystals within N-doped porous carbon nanofibers via electrospinning towards high-performance lithium ion batteries. Nanoscale 8(14):7595–7603. doi:10.1039/c5nr09305h

[132] Zou L, Gan L, Lv RT, Wang MX, Huang ZH, Kang FY, Shen WC (2011) A film of porous carbon nanofibers that contain Sn/SnO*x* nanoparticles in the pores and its electrochemical performance as an anode material for lithium ion batteries. Carbon 49(1):89–95. doi:10.1016/j.carbon.2010.08.046

[133] Zhou D, Lin HM, Zhang F, Niu H, Cui LR, Wang Q, Qu FY (2015) Freestanding MnO_2 nanoflakes/porous carbon nanofibers for high-performance flexible supercapacitor electrodes. Electrochim Acta 161:427–435. doi:10.1016/j.electacta.2015.02.085

[134] McCormac K, Byrd I, Brannen R, Seymour B, Li J, Wu J (2015) Preparation of porous Si and TiO_2 nanofibres using a sulphur-templating method for lithium storage. Phys Status Solidi (a) 212(4):877–881. doi:10.1002/pssa.201431834

[135] Bognitzki M, Czado W, Frese T, Schaper A, Hellwig M, Steinhart M, Greiner A, Wendorff JH (2001) Nanostructured fibers via electrospinning. Adv Mater 13(1):70–72.

doi:10.1002/1521-4095(200101)13:1<70:AID-ADMA70>3.0.CO;2-H

[136] Lin J, Ding B, Yu J (2010) Direct fabrication of highly nanoporous polystyrene fibers via electrospinning. ACS Appl Mater Interfaces 2(2):521–528. doi:10.1021/am900736h

[137] Dayal P, Liu J, Kumar S, Kyu T (2007) Experimental and theoretical investigations of porous structure formation in electrospun fibers. Macromolecules 40(21):7689–7694. doi:10.1021/ma0714181

[138] Li L, Jiang Z, Li MM, Li RS, Fang T (2014) Hierarchically structured PMMA fibers fabricated by electrospinning. RSC Adv 4(95):52973–52985. doi:10.1039/c4ra05385k

[139] Li Y, Lim CT, Kotaki M (2015) Study on structural and mechanical properties of porous PLA nanofibers electrospun by channel-based electrospinning system. Polymer 56:572–580. doi:10.1016/j.polymer.2014.10.073

[140] Zhao JH, Si N, Xu L, Tang XP, Song YH, Sun ZY (2016) Experimental and theoretical study on the electrospinning nanoporous fibers process. Mater Chem Phys 170:294–302. doi:10.1016/j.matchemphys.2015.12.054

[141] Casper CL, Stephens JS, Tassi NG, Chase DB, Rabolt JF (2004) Controlling surface morphology of electrospun polystyrene fibers: effect of humidity and molecular weight in the electrospinning process. Macromolecules 37(2):573–578. doi:10.1021/ma0351975

[142] Huang L, Cheng JL, Qu GX, Li XD, Hu Y, Ni W, Yuan DM, Zhang Y, Wang B (2015) Porous carbon nanofibers formed in situ by electrospinning with a volatile solvent additive into an ice water bath for lithium-sulfur batteries. RSC Adv 5(30):23749–23757. doi:10.1039/c4ra14680h

[143] Kongkhlang T, Kotaki M, Kousaka Y, Umemura T, Nakaya D, Chirachanchai S (2008) Electrospun polyoxymethylene: spinning conditions and its consequent nanoporous nanofiber. Macromolecules 41(13):4746–4752. doi:10.1021/ma800731r

[144] Fashandi H, Karimi M (2012) Pore formation in polystyrene fiber by superimposing temperature and relative humidity of electrospinning atmosphere. Polymer 53(25):5832–5849. doi:10.1016/j.polymer.2012.10.003

[145] Yu XL, Xiang HF, Long YH, Zhao N, Zhang XL, Xu JA (2010) Preparation of porous polyacrylonitrile fibers by electrospinning a ternary system of PAN/DMF/H_2O. Mater Lett 64(22):2407–2409. doi:10.1016/j.matlet.2010.08.006

[146] Shen Z, Hu Y, Chen YL, Zhang XW, Wang KH, Chen RZ (2015) Tin nanoparticle-loaded porous carbon nanofiber composite anodes for high current lithium-ion batteries. J Power Sources 278:660–667. doi:10.1016/j.jpowsour.2014.12.106

[147] Kim C, Yang KS (2003) Electrochemical properties of carbon nanofiber web as an electrode for supercapacitor prepared by electrospinning. Appl Phys Lett 83(6):1216–1218. doi:10.1063/1.1599963

[148] Kim C, Choi Y-O, Lee W-J, Yang K-S (2004) Supercapacitor performances of activated carbon fiber webs prepared by electrospinning of PMDA-ODA poly(amic acid) solutions. Electrochim Acta 50(2–3):883–887. doi:10.1016/j.electacta.2004.02.072

[149] Kim C, Park S-H, Lee W-J, Yang K-S (2004) Characteristics of supercapaitor electrodes of PBI-based carbon nanofiber web prepared by electrospinning. Electrochim Acta 50(2–3):877–881. doi:10.1016/j.electacta.2004.02.071

[150] Kim C (2005) Electrochemical characterization of electrospun activated carbon nanofibres as an electrode in supercapacitors. J Power Sources 142(1–2):382–388. doi:10.1016/j.jpowsour.2004.11.013

[151] Kim BH, Yang KS, Yang DJ (2013) Electrochemical behavior of activated carbon nanofiber-vanadium pentoxide composites for double-layer capacitors. Electrochim Acta 109:859–865. doi:10.1016/j.electacta.2013.07.180

[152] Kim BH, Yang KS (2014) Enhanced electrical capacitance of tetraethyl orthosilicate-derived porous carbon nanofibers produced via electrospinning. J Electroanal Chem 714:92–96. doi:10.1016/j.jelechem.2013.12.019

[153] Nan D, Huang Z-H, Lv R, Yang L, Wang J-G, Shen W, Lin Y, Yu X, Ye L, Sun H, Kang F (2014) Nitrogen-enriched electrospun porous carbon nanofiber networks as high-performance free-standing electrode materials. J Mater Chem A 2(46):19678–19684. doi:10.1039/c4ta03868a

[154] Kim CH, Kim BH (2015) Zinc oxide/activated carbon nanofiber composites for high-performance supercapacitor electrodes. J Power Sources 274:512–520. doi:10.1016/j.jpowsour.2014.10.126

[155] Ra EJ, Raymundo-Pinero E, Lee YH, Beguin F (2009) High power supercapacitors using polyacrylonitrile-based carbon nanofiber paper. Carbon 47(13):2984–2992. doi:10.1016/j.carbon.2009.06.051

[156] Wang G, Pan C, Wang L, Dong Q, Yu C, Zhao Z, Qiu J (2012) Activated carbon nanofiber webs made by electrospinning for capacitive deionization. Electrochim Acta 69(5):65–70. doi:10.1016/j.electacta.2012.02.066

[157] Nie H, Xu C, Zhou W, Wu B, Li X, Liu T, Zhang H (2016) Free-standing thin webs of activated carbon nanofibers by electrospinning for rechargeable Li–O_2 batteries. ACS Appl Mater Interfaces 8(3):1937–1942. doi:10.1021/acsami.5b10088

[158] Zhou ZP, Wu XF (2013) Graphene-beaded carbon nanofibers for use in supercapacitor electrodes: synthesis and electrochemical characterization. J Power Sources 222:410–416. doi:10.1016/j.jpowsour.2012.09.004

[159] Li WH, Li MS, Wang M, Zeng LC, Yu Y (2015) Electrospinning with partially carbonization in air: highly porous carbon nanofibers optimized for high-performance flexible lithium-ion batteries. Nano Energy 13:693–701. doi:10.1016/j.nanoen.2015.03.027

[160] Zhu S, Chen M, Sun J, Liu J, Wu T, Su H, Qu S, Xie Y, Wang S, Su X, Diao G (2016) Novel highly conductive ferroferric oxide/porous carbon nanofiber composites prepared by electrospinning as anode materials for high performance Li-ion batteries. RSC Adv 6(63):58529–58540. doi:10.1039/c6ra04090j

[161] Ma C, Li YJ, Shi JL, Song Y, Liu L (2014) High-performance supercapacitor electrodes based on porous flexible carbon nanofiber paper treated by surface chemical etching. Chem Eng J 249:216–225. doi:10.1016/j.cej.2014.03.083

[162] Kim C, Ngoc BTN, Yang KS, Kojima M, Kim YA, Kim YJ, Endo M, Yang SC (2007) Self-sustained thin webs consisting of porous carbon nanofibers for supercapacitors via the electrospinning of polyacrylonitrile solutions containing zinc chloride. Adv Mater 19(17):2341–2346. doi:10.1002/adma.200602184

[163] Jing LI, Lai YQ, Zhao XD, Peng RF, Liu YX (2011) Electrochemical performance of carbon electrode materials prepared by different activated methods. J Southwest Univ Sci Technol 1:004